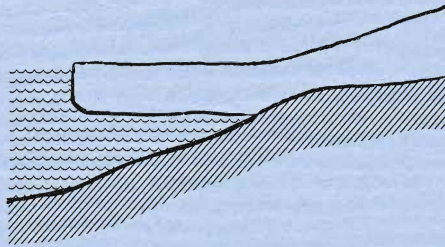




SKRIFTER NR. 187

---

Glaciological research on  
Riiser-Larsenisen and nearby ice-shelves  
in Antarctica



---

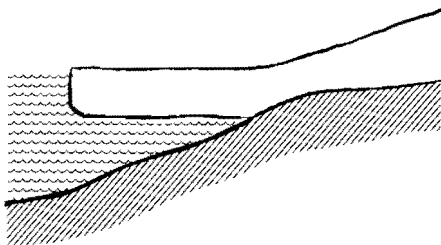
NORSK POLARINSTITUTT  
OSLO 1986



SKRIFTER NR. 187

---

Glaciological research on  
Riiser-Larsenisen and nearby ice-shelves  
in Antarctica



---

NORSK POLARINSTITUTT  
OSLO 1986

ISBN 82-90307-45-4  
Printed December 1986

## Contents

Preface .....	4
Orheim, Olav: Flow and thickness of Riiser-Larsenisen, Antarctica .....	5
Appendix: Drewry, David: SPRI radio echo sounding of Riiser-Larsenisen .....	21
Gjessing, Yngvar & Wold, Bjørn: Absolute movements, mass balance and snow temperatures of the Riiser-Larsenisen Ice Shelf, Antarctica .....	23
Orheim, O., Gjessing, Y., Lunde, T., Repp, K., Wold, B., Clausen, H. B. & Liestøl, O.: Oxygen isotopes and accumulation rates at Riiser-Larsenisen, Antarctica .....	33

# Preface

Riiser-Larsenisen is a 100 km wide ice shelf in western Dronning Maud Land. Oblique aerial photographs of the area were collected during the 1950/51, 1951/52 and 1958/59 summer seasons, by flights from Maudheim and from Norway Station. The first glaciological investigations by Norwegian researchers were done in 1968/69. These were followed by larger dedicated glaciological programmes during the Norwegian Antarctic Research Expeditions 1976/77 and 1978/79. Most of the results from these studies are reported here in three articles which discuss ice thicknesses, flow rates and other flow phenomena, accumulation rates and the mass balance of the ice shelf, snow temperatures, and results of various isotopic studies.

It was desired to collect the three articles presented here in one volume. This, combined with late completion of the article by Orheim et al.: 'Oxygen isotopes and accumulation rates at Riiser-Larsenisen, Antarctica', unfortunately resulted in a considerably delayed publication of the other two articles.

*November 1986*

*Olav Orheim*

OLAVORHEIM:

# Flow and thickness of Riiser-Larsenisen, Antarctica\*

*with an Appendix by David Drewry, Scott Polar Research Institute*

Orheim, O. 1986: Flow and thickness of Riiser-Larsenisen, Antarctica. *Norsk Polarinstitutt Skrifter* 187, 5–22.

The Norwegian Antarctic Research Expedition (NARE) 1978/79 used the SPRI Mk IV System fitted in a helicopter to fly 620 km radio echo sounding over the central part of Riiser-Larsenisen, and 100 km across the outer part of Stancomb-Wills Ice Stream. Observed thicknesses of Riiser-Larsenisen decrease from a maximum of 650 m a few km from the grounding line to less than 200 m at the ice front. The Kvitkuven ice rise shows thicknesses between 200 m and 500 m. The thickness data suggest that the ice shelf east of Kvitkuven turns clockwise and flows obliquely to the ice front. Comparison of positions of the ice front based on 1974 Landsat imagery and NARE 1977 and 1979 surveys indicates minimum ice front velocities ranging from 200 m a<sup>-1</sup> to 700 m a<sup>-1</sup>. The surveys also show that three large sections of the ice shelf east of Kvitkuven broke away at different periods between 1974 and 1979. Each of these was around 10 km × 20 km, and their total area exceeded 650 km<sup>2</sup>.

The radio echo sounding indicates that the ice shelf has a complex flow regime. Steplike change in thickness of > 150 m over a 500 m horizontal distance is observed in the central part of the ice shelf. The records also demonstrate undulations in ice thickness and bottom morphology of 600–700 m wavelength and 50 m amplitude, and various types of rifts and crevasses. Internal layering is recorded at 250–300 m depth within the Kvitkuven ice rise and in the ice shelf upstream of the ice rise.

Combination of the NARE data with radio echo sounding data from 1970, provided from the Scott Polar Research Institute, shows that Riiser-Larsenisen has an average thickness of around 300 m, with generally larger thicknesses west of Kvitkuven. The bulk of the inland ice around Vestfjella is 700 m–1200 m thick.

Observed ice thicknesses of Stancomb-Wills Ice Stream range from 135 to 241 m, with no systematic decrease towards the ice front. The records include long sections of numerous reflecting hyperbolas from densely spaced rifts and bottom crevasses. This ice stream attains velocities > 4 km a<sup>-1</sup>, and the high activity has resulted in extensive fracturing.

*O. Orheim, Norsk Polarinstitutt, P.O. Box 158, 1330 Oslo Lufthavn, Norway.*

The glaciological programme of the Norwegian Antarctic Research Expedition (NARE) 1978/79 included radio echo sounding of icebergs and ice shelves. We used the Scott Polar Research Institute (SPRI) Mk IV System, operating at a centre frequency of 60 MHz (see e.g. Evans & Smith 1969). The equipment was mounted in the rear compartment of a Bell 206B (Jetranger) helicopter. It consisted of the 60 MHz unit fitted with a Honeywell oscillograph visicorder including a heat processing unit for high quality permanent records. This left just enough room for an operator in the rear. A navigator flew in the front compartment with the pilot. The antenna was a simple 3.8 m dipole, provided by the Technical

University of Denmark, mounted parallel to the helicopter body at a distance of 2 m, using fibre-glass supports.

A little more than 10 hours of radio echo sounding were flown on the expedition. This included 1) soundings of nine icebergs (Orheim 1980), 2) some flights with poor navigation near Halley on the Brunt Ice Shelf and on the Filchner Ice Shelf, and 3) flights of Riiser-Larsenisen and Stancomb-Wills Ice Stream (Fig. 1). The results of 3) are reported here.

Flights were mostly flown at speeds of 160–180 km/h, and at elevations of either ≈ 20 m or ≈ 350 m above the surface. Three radio echo sounding flights of Riiser-Larsenisen covered 620 km (Fig.

\* *Publication No. 49 of the Norwegian Antarctic Research Expeditions (1978/79).*

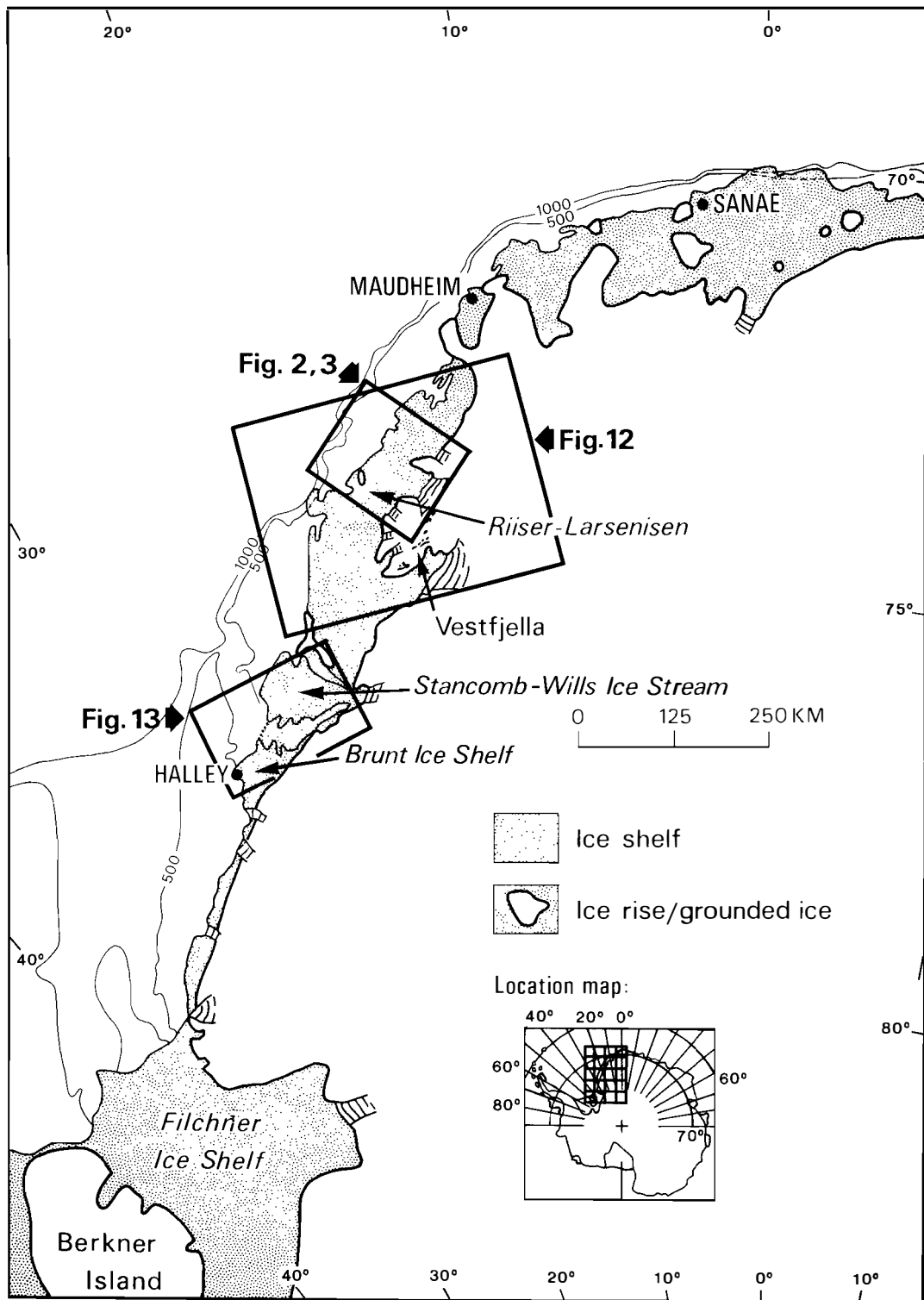


Fig. 1. Index map of studied areas.

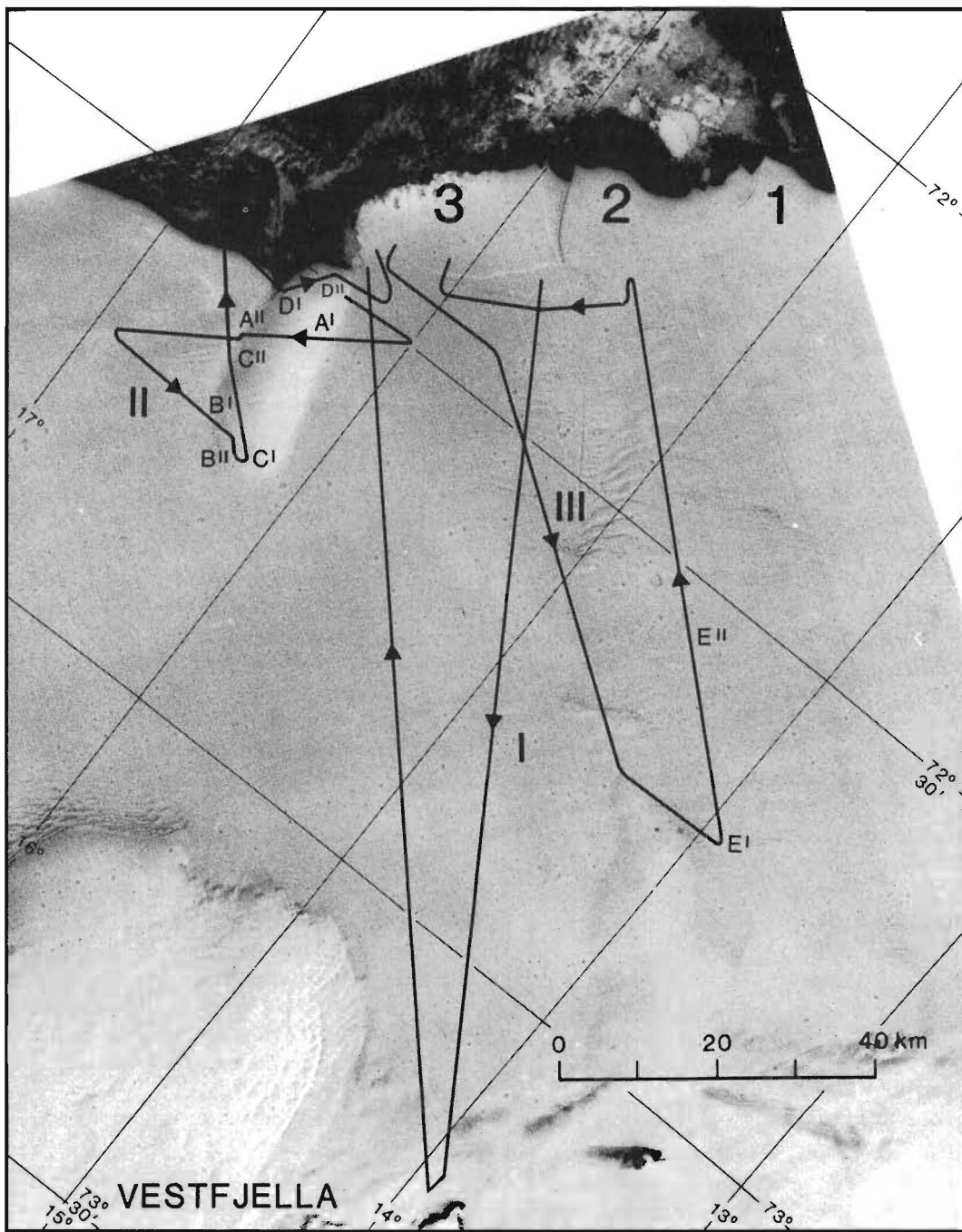


Fig. 2. Part of Landsat imagery 1544-08325, from 18 January 1974, showing physiographic features of Riiser-Larsenisen, and segments 1-3 that broke off between 1974 and 1979. The radio echo flights are marked I, II, and III, with letters that refer to sections described in the text.

2), as part of a glaciological programme to study this ice shelf, carried out during NARE 1976/77 and 1978/79 (Repp 1978; Gjessing 1984; Gjessing & Wold 1986; Orheim et al. 1986).

## Data reduction

### *Ice thickness and altitude*

The ice thicknesses are calculated in m from the formula

$$169 \times T + 10,$$

where T is the one-way travel time in  $\mu\text{s}$ . The velocity of radar in ice is taken as  $169 \text{ m } \mu\text{s}^{-1}$ , and 10 m is added to the directly computed ice thickness to compensate for the higher velocity in the upper firm layer of lower density (e.g. Neal 1979).

The one-way travel time could be read to 0.02  $\mu\text{s}$  directly from the paper charts without magnification. Ice thicknesses were read from the records at flight distance spacing mostly between 0.7 and 1.0 km.

The helicopter was fitted with both radar and pressure altimeters. The surface echo was masked when we flew at low elevations (20 m), but at these times the flying height was recorded from the instruments by the navigator to  $\pm 3$  m. The flight level accuracy is probably 10–20 m when flying at high elevations. The errors in ice thickness are probably less than 10 m in cases of good bottom echoes.

### *Navigation*

Navigation on the Riiser-Larsen flights was mainly achieved by 'dead reckoning' at fixed headings for known topographic landmarks. The latter included mountain peaks when flying towards Vestfjella, and a homing signal towards the ship. The first flight (I, Fig. 2) suffered from intermittent equipment failure, and some minute-marks were not recorded. This made the navigation less certain. On the other hand, the use of the Honeywell system enabled the operator to mark pertinent events (helicopter turns, crevasses, etc.) directly on the paper chart. This gave added control of the subsequent matching of the sounding records with navigation data.

The navigation uncertainties are probably 1–5 km for flight I, and 0.5 to 2 km for flights II and III. On flight I the main uncertainties concern

positioning *along* the shown track because of the time signal failures.

Navigation on the Stancomb-Wills Ice Stream flight was based on the known starting- and termination-points by the ship, located near the ice front. The track was then reconstructed from the flight navigation data and by assuming constant wind during the 30 minutes of the flight.

## Results

### *Thickness of Riiser-Larsenisen*

The ice thickness map (Fig. 3) covers the central part of Riiser-Larsenisen from  $14^\circ \text{W}$  to  $17^\circ \text{W}$ . West of Kvitkuven the ice thickness decreases fairly regularly towards the ice front, whereas this is not the case east of Kvitkuven. Here the thickness contours indicate that the main ice flow turns clockwise in the central part of the shelf and possibly crosses the ice front obliquely over a section east of  $15^\circ 30' \text{W}$ . There are unfortunately no velocity measurements from the central part to check this. The thinner ice further east may be an effect of the more elevated bedrock around  $72^\circ 40' \text{S}$ ,  $14^\circ 30' \text{W}$ , where the grounding line extends to within 50 km of the ice front. An oval-shaped closed ice-thickness minimum is located northwest of this grounding line. The amplitude is about 110 m, similar to the largest described from the Ross Ice Shelf (Bentley et al. 1979). The high thickness gradient of  $> 10 \text{ m/km}$  in the central area of the ice shelf where the flow turns clockwise suggests a thinning and acceleration of the ice shelf, perhaps related to channeling of the ice flow. The ice thickness along a stake line established in 1977 (Fig. 3) decreases from 650 m, at a few km from the grounding line, to 220 m at the ice front.

The ice front exhibits the greatest thicknesses just east of Kvitkuven (Fig. 3). This can be explained as a lack of ice shelf adjustment related to the 1977–79 calving of this part of the ice shelf, described below.

### *Changes in ice front position and flow rates*

The positions of the ice front of Riiser-Larsenisen have been determined from a January 1974 Landsat image and from the ship tracks with high

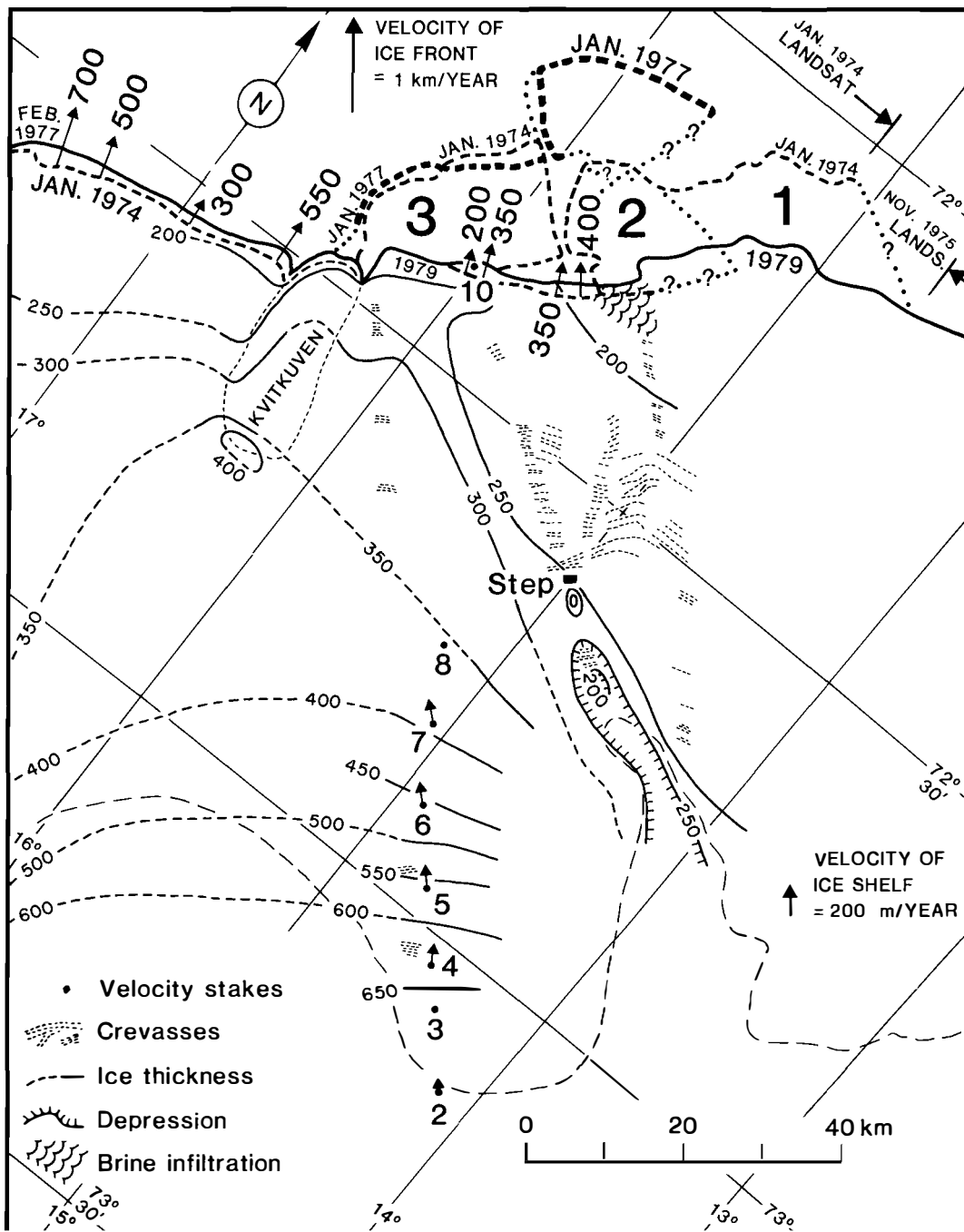


Fig. 3. Ice thickness contours of Riser-Larsenisen at 50 m intervals. Also shown are crevasses recorded visually and on radio echo soundings, zone of brine infiltration, and the grounding line (thin dashed line). The location of the ice front at various times between 1974 and 1979 is given together with minimum ice front velocities, and Gjessing & Wold's (1986) stake velocity determinations.

precision navigation in January/February 1977 and February 1979. They are shown in Fig. 3. The Landsat image is shown in Fig. 2, and on this are also marked the three sections: '1' that broke off between 1974 and 1977, '2' which separated in 1977, and '3' which calved off between 1977 and 1979.

Section 1 had disappeared before our survey in January 1977. The eastern limit of the section cannot be determined, as the 1974 Landsat image does not extend east of  $15^{\circ} 10' W$ , and as there are no adjoining Landsat images or other relevant surveys for this period. The nearest Landsat image has its western limit at  $14^{\circ} 35' W$ , and the position of the coast is close to our 1977 and 1979 ice front surveys. This image is from November 1975.

Comparison of the 1974 Landsat image and the 1977 NARE ice front surveys and field party observations shows that section 2 had broken off from the ice shelf, and was in the process of moving away from the coast, in January 1977. Our survey on 15 January showed that the section had moved out about 15 km, compared with the 1974 position, and rotated  $20^{\circ}$  anti-clockwise. The segment was in the process of moving clear of section 3 on the western side, with less than 3 km of overlap remaining between the two sides. It was at that time also bound by annual and multiyear sea ice on its eastern side. The segment separated completely from the coast around 10 February during strong winds, and we observed it drifting with the westerly shore current when the ice front was resurveyed on 15 February.

Section 3 broke off sometime between March 1977 and our revisit in February 1979.

Sections 1, 2 and 3 that calved off measured about  $22(?) \text{ km} \times 11(?) \text{ km}$ ,  $23 \text{ km} \times 16(?) \text{ km}$  (in triangular(?) shape), and  $24 \text{ km} \times 12 \text{ km}$  respectively. None of these sections were recorded on the weekly sea ice maps for the relevant periods. These maps are produced by the U.S. Navy/NOAA Joint Ice Center, where they try to record all icebergs with major axes  $> 27 \text{ km}$ . The failure to record the calved icebergs may have been due to their being just below this limit, or because they quickly broke into smaller parts.

There is no evidence of large iceberg calvings west of Kvitkuven between 1974 and 1977. The *minimum* flow rates of the ice front for this inter-

val can be determined by comparing the change in position of the ice front. This method gives rates between  $300 \text{ ma}^{-1}$  and  $700 \text{ ma}^{-1}$ , with the highest velocity furthest away from Kvitkuven (Fig. 3). Any calvings in the interval will reduce the expansion of the ice front and thus lead to apparent velocities that are lower than reality. The relatively low velocities in the middle of the section are likely to be the result of a segment of the ice shelf having calved away.

East of Kvitkuven, across section 3, the determination of the flow rate depends upon fixing the line of break-off of the section. This probably took place along the marked rift observed in the Landsat image (Fig. 2), and this is supported by the observations of the field parties. The minimum velocities of this part of the ice front for the 1974–79 period are then found to increase eastwards away from Kvitkuven, from  $200 \text{ ma}^{-1}$  and  $350 \text{ ma}^{-1}$ , respectively, just west and east of stake 10, to  $350 \text{ ma}^{-1}$  and  $400 \text{ ma}^{-1}$  near the rift separating sections 2 and 3 in Fig. 2. East of this rift the flow rate cannot be determined because the line of fracture cannot be reconstructed with confidence.

The uncertainty in these minimum ice front velocities based on repeated surveying is mainly determined by the uncertainty in positioning, which for this area varies from 200–400 m west of Kvitkuven, to 100–300 m on the east side. This gives a probable error in the minimum velocities of  $100\text{--}200 \text{ ma}^{-1}$ , with the largest uncertainties in the velocities west of Kvitkuven, both because of larger uncertainties in the positions and because of shorter time interval between the surveys.

The above velocities determined from repeated surveying of the ice front are higher than the ice front velocity for the 1977–79 period obtained by Gjessing & Wold (1986). They measured  $110 \text{ ma}^{-1}$  at stake 10 by surveying from Kvitkuven and by assuming the direction of flow to be perpendicular to the ice front. They also measured annual flow between 30 and 130 m at locations along the stake line from 2 to 7 (Fig. 3) by triangulation from rock. Their value at stake 10 seems low both in view of their measurements of higher upstream velocities and in view of the ice front surveys.

We may consider whether the break-off of the

ice shelf east of Kvitkuven would lead to acceleration of the adjoining upstream shelf due to increased creep deformation, and therefore to abnormally high velocities for the years up to 1979. We do not have sufficient data from Riiser-Larsenisen to calculate the increased velocity due to the reduced back pressure. However, if we assume the ice front conditions here to be like those at the Ross Ice Shelf, then we can calculate from data and considerations presented by Thomas & MacAyeal (1982) that calving off of 10+ km wide sections should lead to maximum 20% velocity increase of the adjoining ice shelf. Thus, this effect is not likely to cause large deviations from the multi-year mean velocity of the ice front.

### *Ice rises*

The area contains one prominent ice rise, Kvitkuven, which measures 10 × 30 km. Four profiles across it (Fig. 4) show ice thicknesses between 200 m and 500 m and fairly symmetrical surface profiles despite asymmetrical bedrock. The largest thicknesses are found at the southern boundary, where there is a local ice thickness maximum caused by Kvitkuven blocking the flow of the ice shelf. The ice thickness of Kvitkuven is generally greater than at the adjoining ice shelf.

The ice shelf both increases in thickness and shows surface depressions as it flows against the ice rise (Figs. 4 and 5). Autenboer & Declair (1972) described similar phenomena from the Jelbartisen-Fimbulisen area. They agreed with Swithinbank's (1957) explanation that the ice exhibits persistence of downward movement. It is difficult to visualize how this can take place over distances exceeding one km and with ice thicknesses increasing by >100 m, as shown here. I suggest that the ice rise 'dams' the ice flow, causing larger thicknesses and stresses at its upstream end, and further that the associated surface depressions are effects of rifts that form around the ice rise because of longitudinal strain. These probably continue both to be enlarged by flow and to be filled with drift snow.

### *Undulations*

The flight section from E' to E'' (Fig. 2) crossed nearly normal to surface undulations, and here

the ice thickness showed spatial variations (Figs. 6 and 7) exceeding 50 m with wavelengths of 600–700 m. The undulations were recorded on a low-flying portion of the survey, and the surface echo was not recorded. They were observed as waves on the ice surface, but the subsequent matching of the radio echo sounding records with the recordings of flight elevation and terrain clearance showed that the latter were not recorded with sufficient frequency to allow determination of the upper surface form of the waves. The observed surface elevation variations across the waves had a maximum amplitude of 5–7 m, which agree well with what would be expected if the ice was isostatically adjusted. However, whether this really was the case cannot be ascertained. In Fig. 7 the undulations are reproduced as thickness variations, with the mean surface shown as a straight line.

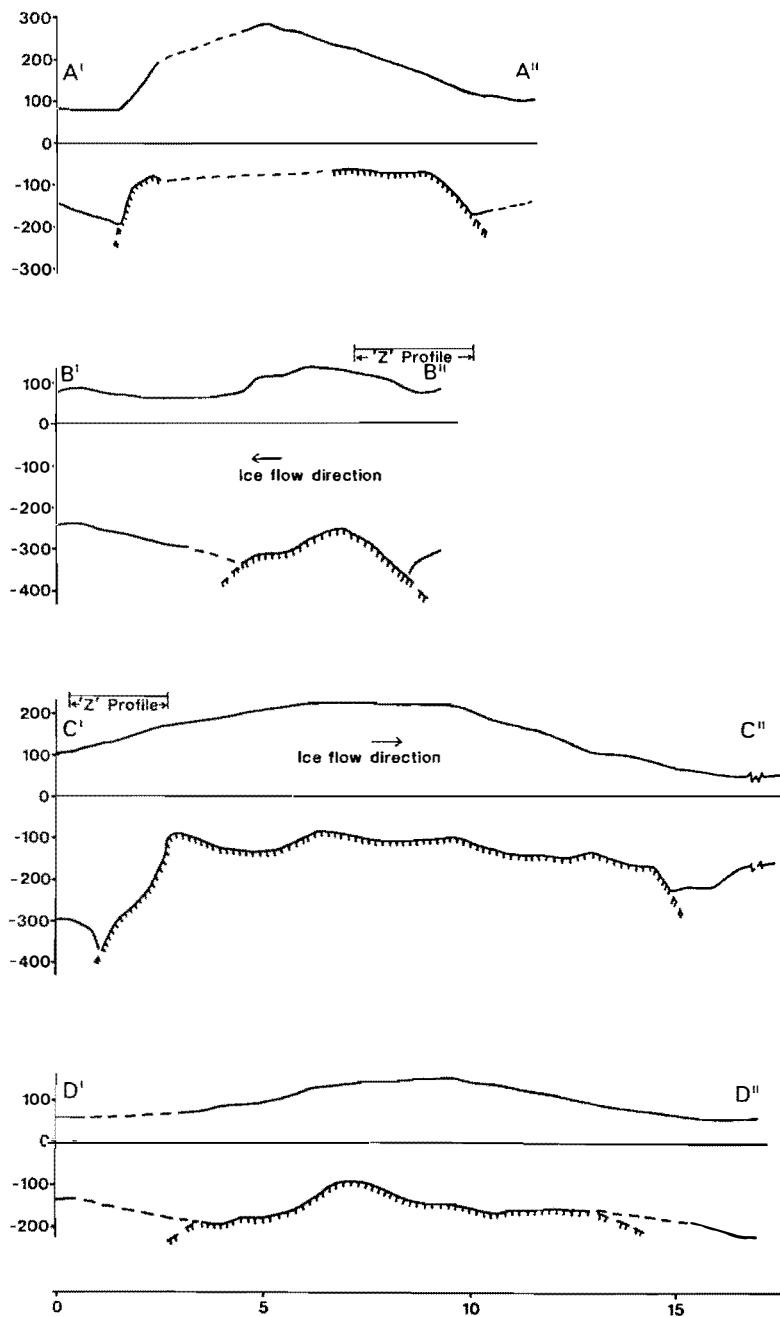
The waves form approximately at the grounding line. They are slightly asymmetric and decrease in amplitude downstream until they become indistinguishable in the record after 30 km. The near-by ice velocity measurements by Gjesing & Wold (1986) give  $120 \text{ m a}^{-1}$ . The undulations are probably several motion-years apart, and they probably span a time interval of >100 years.

The origin of the waves is not known. Possibly, they are caused by longitudinal strain on the grounded ice resulting from faster flowing ice on the south-western side, with a spacing that may be related to the ice thickness of approximately 250 m, and/or to pre-existing flaws.

As the ice shelf segment moves downstream, the undulations decrease in amplitude, possibly resulting from effects both at the surface and at the base. An excess accumulation of 0.05 m in the hollows compared with the ridges would dampen surface waves of 5 m amplitude within 100 years. The mean balance at Riiser-Larsenisen is 0.4 m water equivalent. Thus such an excess represents a variation in accumulation of <10% across the undulations. Such, and much larger variations in accumulation with topography, can result from the effects of snow drift and are well known, e.g. Gow & Rowland (1965).

At the base the undulations can be smoothed by melting/freezing processes associated with ocean currents flowing across the topography. A water mass crossing the topography will be in

Fig. 4. Profiles across Kvitkuven. For location, see Fig. 2. Thin bottom line shows floating ice shelf, hatched line shows grounded ice/rock interface. Distances in km. Vertical scale in m, 10 times exaggeration.



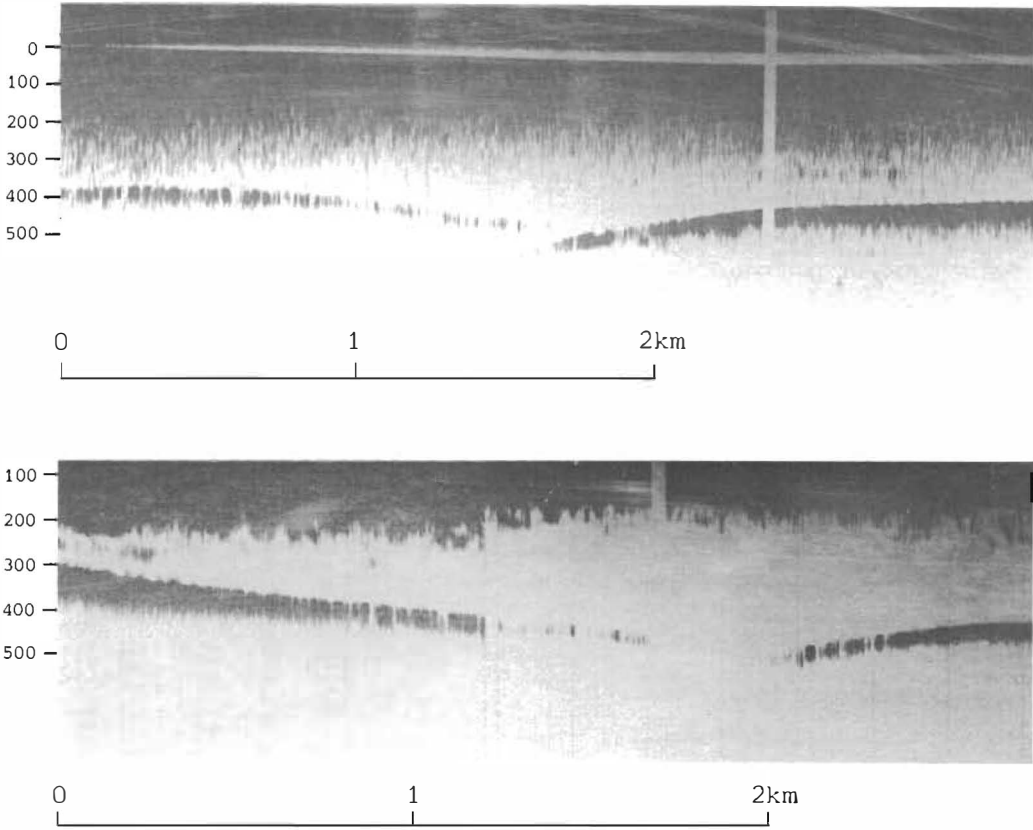


Fig. 5. Radio echo sounding 'Z' profiles of the ice shelf/Kvitkuven contact. Above: From location B'' in Fig. 2. Below: From C'. Iceflow from right to left. Vertical exaggeration  $\approx 25\%$ .

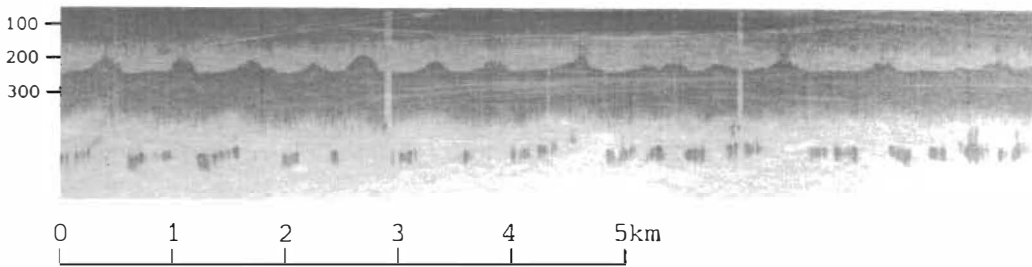


Fig. 6. 'Z' profile of bottom undulations, from central section of E'-E'' in Fig. 2. Note that the surface signal is not shown. Left hand scale shows ice thickness in m. Vertical exaggeration  $\approx 3$  times.

disequilibrium with the pressure melting point of the basal ice. It will melt off the thicker ice and freeze on new ice at shallower depths (Doake 1976; Robin 1979). The record (Fig. 7) shows that multiple reflections are recorded only from the thick ice, indicating that the absorption of the radio echo waves is higher for the thin ice. It seems likely that the explanation for this higher dielectric loss is the presence of saline ice resulting from frozen-on sea water, as discussed by Neal (1979). Correspondingly, the regions of thick ice with high reflection coefficients are believed to represent zones of local bottom melting. The calculations by Robin (1979) show that a differential melting/freezing of 50 m is quite plausible in a time span of 100 years.

Such undulations were observed only at this one section of the record. Large longitudinal strains will more commonly lead to total fracture, as discussed below.

### *Rifts and crevasses*

Rifts, with widths sometimes exceeding 1 km, were observed at many localities. They often appeared as marked surface depressions of 10–20 m on the ice shelf and are readily seen in the sounding records. Often the basal signal may be obscured by numerous bottom and surface reflectors (Fig. 8).

The rifts are believed to be caused by longitudinal strain on slower moving ice accelerated by bounding, faster flowing ice streams, and/or strain associated with change in flow direction and with grounding. They have been described in many localities where the inland ice comes afloat, giving rise to a 'normal' thickness ice shelf separated by ice at elevations near sea level, e.g. Brunt Ice Shelf (Thomas 1973).

Bottom crevasses were commonly observed (Fig. 9), particularly around Kvitkuven and on flight III, and often showed in the records with a trio of hyperbolas reflected from the apex and the bottom corners of the crevasses, as described by Jezek & Bentley (1983) from the Ross Ice Shelf. The largest crevasses were recorded just NW of 'III' in Fig. 2. These were up to 100–200 m wide at the base and in places extended towards the surface through more than 2/3 of the ice thickness.

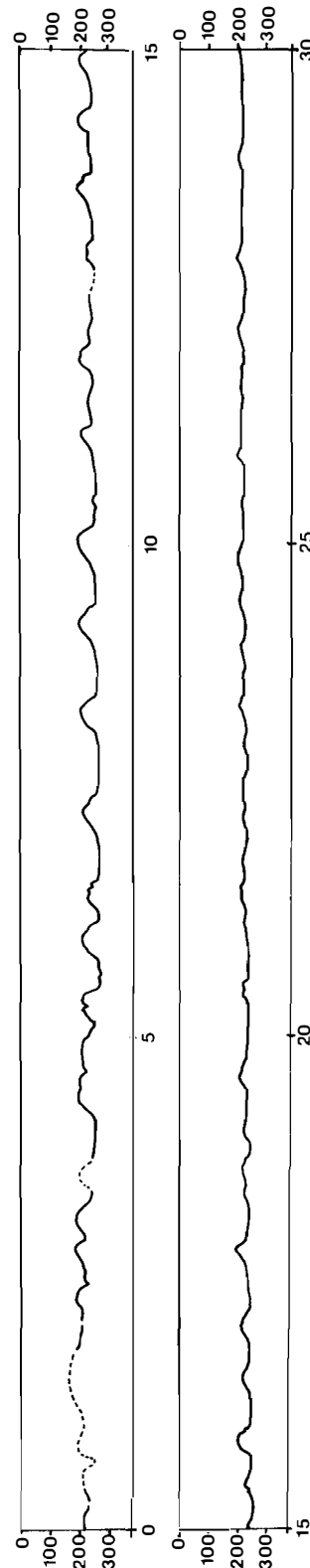


Fig. 7. Variation in ice shelf thickness along the 30 km long section E'-E'' (Figs. 2 and 6), drawn as deviations from a level upper surface.

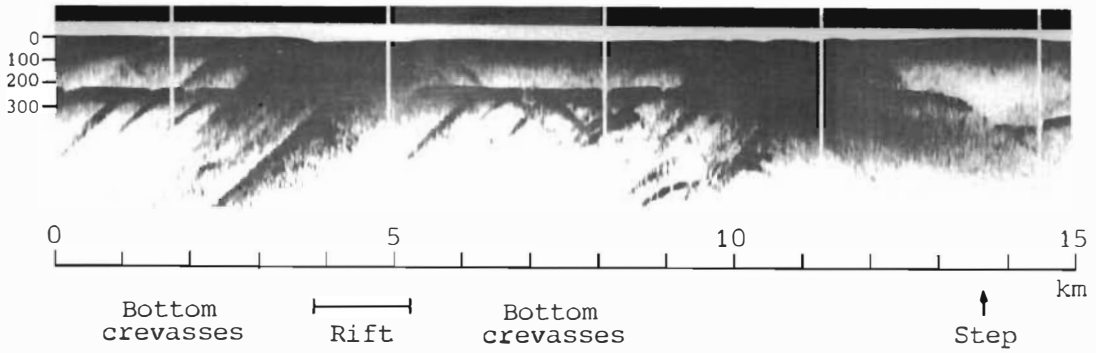


Fig. 8. 'Z' profile section with rifts and surface and bottom crevasses which generate reflections. A step-like change in ice thickness is also shown. Ice flow is from right to left, and the section is near 'III' in Fig. 2.

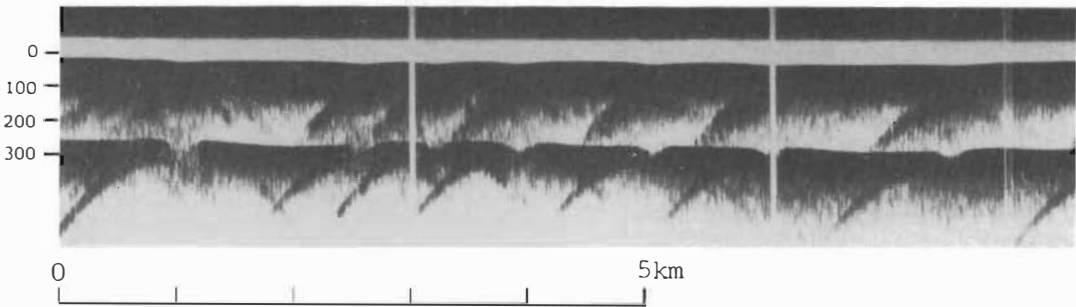


Fig. 9. Examples of large bottom crevasses, located 10–15 km NW of the large rift shown in Fig. 8.

All observed surface and bottom crevasses, apart from the marginal zones of Kvitkuven, are shown in Fig. 3. Altogether more than 50 such crevasses were observed in the ice shelf east of Kvitkuven. It is probable that additional crevasses were present during flight I without being recorded due to the intermittent equipment failure. No crevasses were observed in the ice shelf west of Kvitkuven. Although the flights covered much smaller areas in this part of Riiser-Larsenisen, the distribution of crevasses suggests that the ice flow is more complex east of the ice rise.

*Step-like changes in ice thickness*

Rapid changes in ice thickness are observed upstream of Kvitkuven and southeast of 'III' in the central part of the ice shelf (Figs. 8 and 10). The latter locality shows a > 150 m change in

thickness over a horizontal distance of 500 m. These steps seem to be larger than those from the Ross Ice Shelf, described briefly by Bentley et al. (1979). The records indicate that the ice shelf is *not* grounded, although this cannot be ascertained for the whole section because the echoes from the base are obscured by numerous reflecting hyperbolas. However, heavy crevassing east of this locality suggests possible grounding here.

*Brine infiltration and internal layering*

The signal from the base was lost, without signs of hyperbolas being generated from corner reflectors, in some places near the ice front, mainly in one area (Fig. 3). The echoes are believed occluded as a result of brine infiltration from sea water that has entered the permeable firn through rifts and crevasses. No evidence was

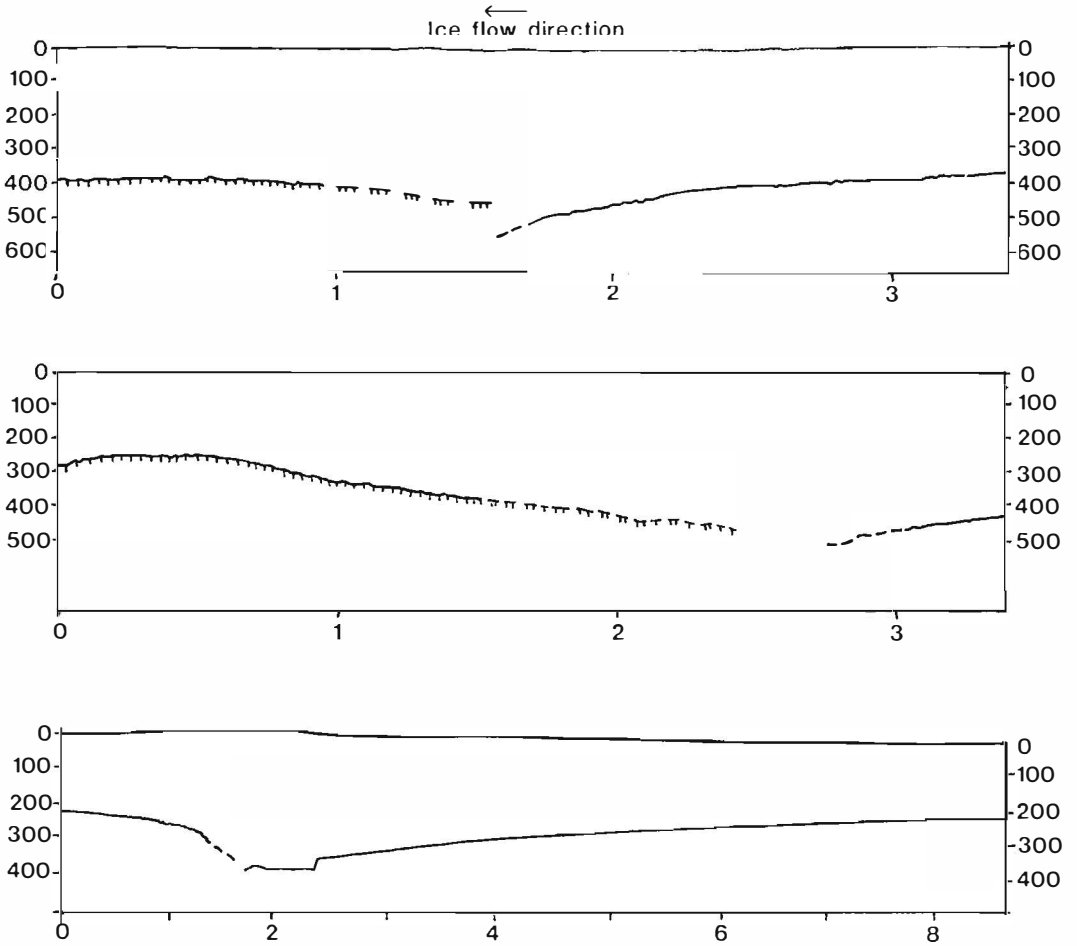


Fig. 10. Profiles showing 'steps' in ice thickness. Upper and middle figures are located at B'' and C', respectively (Fig. 2). They correspond to Fig. 5 and are enlarged portions of Fig. 4. Note that the middle figure is reversed from Fig. 4. The lower figure is from III in Fig. 2 and from 0-3 km it corresponds to the 13-16 km position in Fig. 8. Hatched line shows grounded ice. Upper and lower figure show both upper surface and base of the ice. The middle figure shows only variation in ice thickness drawn as deviation from a level upper surface. Vertical scale in m, horizontal in km. Vertical exaggeration 25 % for upper and middle figure, 3 times for lower figure.

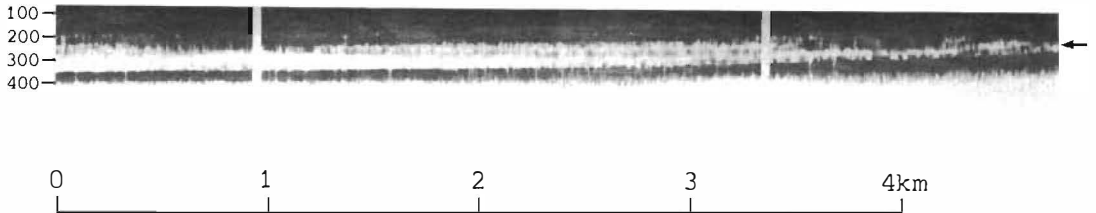


Fig. 11. 'Z' profile of internal layering (arrow) in Kvitkuven, from the southern part of section C'-C''. Ice is mostly grounded.

found in the records of a brine infiltration layer, such as that from the Larsen Ice Shelf described by Smith & Evans (1972).

We observed weak internal layering at 200–300 m depth at different sections over Kvitkuven (Fig. 11) and in the ice shelf just south of the ice rise. The origin of the layers is unknown, but they are not likely to have been caused by brine infiltration. The layers do not attenuate the signal such as described above. Furthermore, all the layers are at depths corresponding to solid ice, whereas brine infiltration layers are usually found in the permeable firm. If the layers are isochrones in the accumulation record resulting from past events, then simple considerations of mass balance and strain indicate that they are  $\approx 500$ –1000 years old.

#### *Additional radio echo soundings of Riiser-Larsenisen*

Part of Riiser-Larsenisen was sounded in January 1970 as part of a joint radio echo sounding programme between the Scott Polar Research Institute (SPRI), Cambridge, UK, and the U. S. National Science Foundation. These studies are described in the Appendix by Dr. David Drewry, SPRI.

Fig. 12 shows the ice thickness of Riiser-Larsenisen and adjoining inland areas based on the combined data from SPRI and the NARE surveys. It shows that the segment of the ice shelf that flows east of Kvitkuven is about 100 m thinner than the ice shelf west of Kvitkuven at equal distance from the front. The bulk of the ice shelf is around 300 m thick, thinning to less than 200 m along the ice front on the easternmost section. The effect of Kvitkuven on the ice shelf thickness is clearly seen, as is the effect of a small ice rise near the ice front at  $18^\circ$  W. Inland of the grounding line the ice thickness is mostly between 700 m and 1200 m.

#### *Comparison with Stancomb-Wills Ice Stream*

100 km of radio echo soundings were flown over the outer, marginal part of the Stancomb-Wills Ice Stream (Fig. 13). The records differed considerably from those at Riiser-Larsenisen. The observed ice thicknesses ranged from 135 m to 241 m, with no systematic decrease towards the

ice front, although thickness could not be determined over long sections because the basal echo was masked by hyperbolas from numerous surface and bottom reflectors, in part off to the side from the helicopter (Fig. 14). Fig. 13 includes six thickness determinations at the southern part of the ice stream, from the SPRI measurements described in the Appendix. These show no systematic variations either.

Fig. 13 also shows minimum ice front velocities determined by comparing positions of the ice front in 1973 from Landsat images, and four years later from NARE 76/77 surveys. Velocities determined by Thomas (1973) are also shown. The ice front surveys show that the outer part of the ice stream attains velocities of 1 to  $>4$  km  $a^{-1}$ , making it among the fastest-flowing Antarctic ice streams. The outer part of the ice stream is in fact formed by agglomeration of blocks of ice shelf, after initial fracture near the grounding line by high longitudinal strain.

## Conclusions

The radio echo soundings of Riiser-Larsenisen have revealed an ice shelf of high dynamic activity, with rifts and bottom and surface crevasses and undulations, and showing rapid changes in ice thickness. Clearly the ice shelf is not made up of level ice of regularly changing thickness and with a simple flow regime. The ice shelf flow is split by Kvitkuven, with one branch flowing north-west from the grounding line at around  $14^\circ 10'W$ , and then turning north to north-northeast at about  $15^\circ 40'W$ . This branch shows a complex flow regime. The other branch, flowing west of Kvitkuven, seems to have a simpler flow, directed at right angles to the ice front.

## Acknowledgements

I am very grateful to Kjell Nythun, who had the technical responsibility for the radio echo sounding, for very good field cooperation. Dr. David Drewry made very useful comments to this paper. The Scott Polar Research Institute, University of Cambridge, very kindly lent us their equipment.

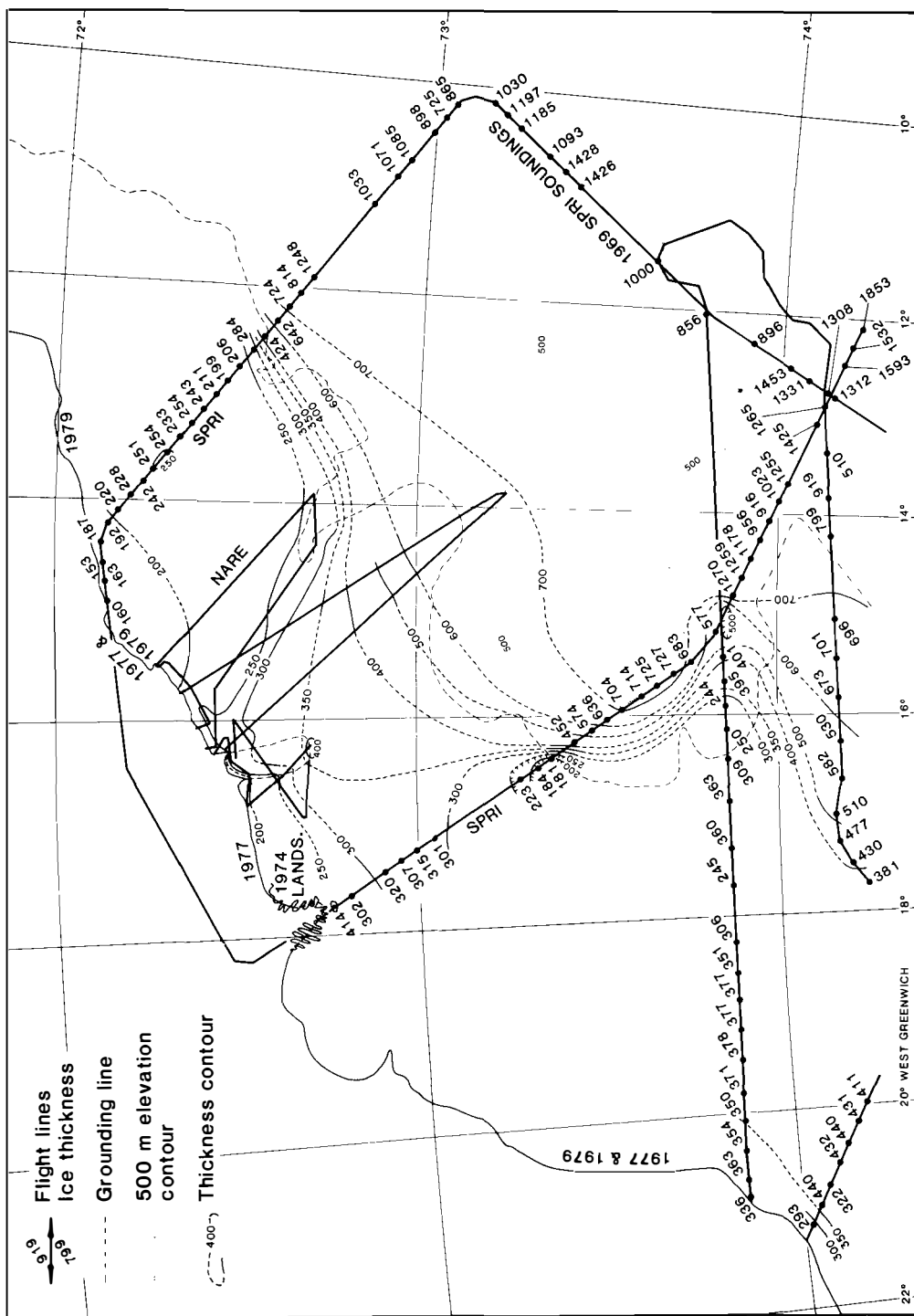


Fig. 12. Flight lines and the ice thickness determinations by SPRI/NSF in 1970 (see Appendix) in combination with the NARE results. Also shown is the grounding line and the 500 m elevation contour, the latter based on Norsk Polarinstiut's maps of Vestfjella. Thickness contours are at 50 m intervals up to 400 m, and 100 m between 400 m and 700 m thickness.

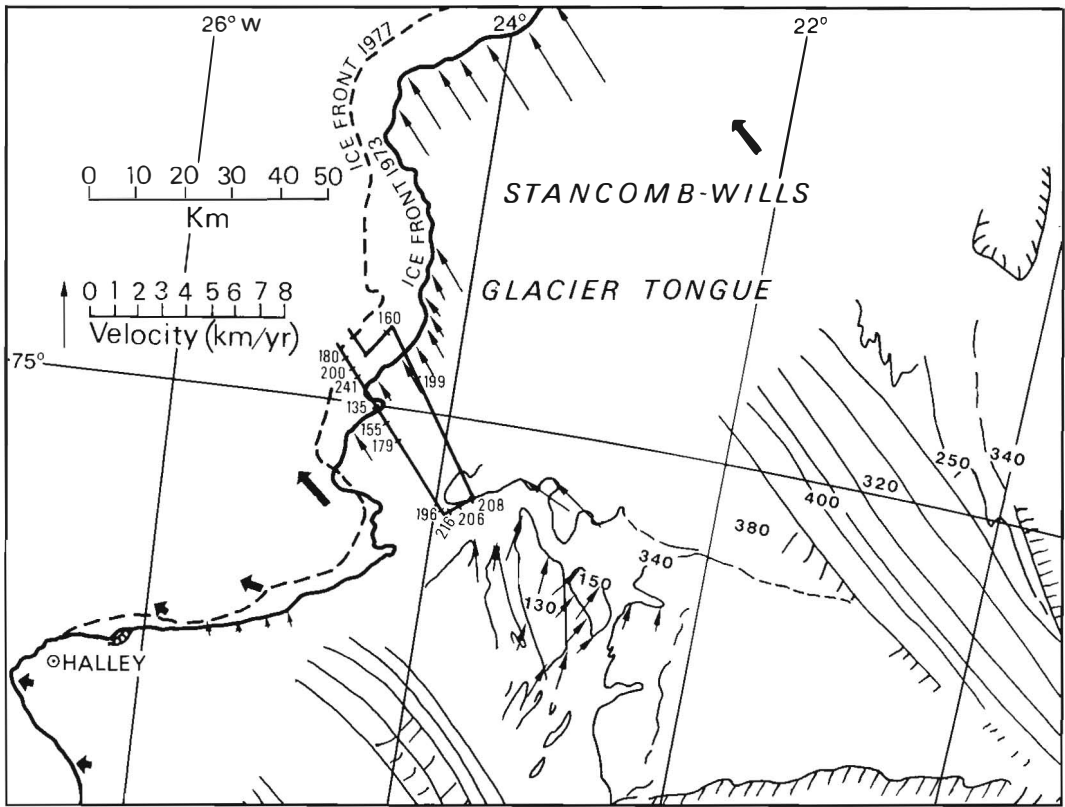


Fig. 13. Map of Stancomb-Wills Ice Stream. The radio echo sounding profile with measured ice thicknesses is shown as solid lines around 75°S, 24°W. Numbers in southern part of ice stream are thicknesses measured by SPRI (see Appendix). The arrows show velocities of different part of the ice shelf. Thin arrows are based on comparison between the 1973 Landsat image and the NARE 1977 ship survey. Thick arrows show ground survey velocities given by Thomas (1973). Velocities within the southwestern part of the ice stream are based on displacements of ice shelf segments ('ice bergs') determined by comparing the map by Thomas (1973) with Landsat image I188-09002 of 27 January 1977. Thin lines indicate flow lines and crevasses. Hatched lines mark grounded areas.

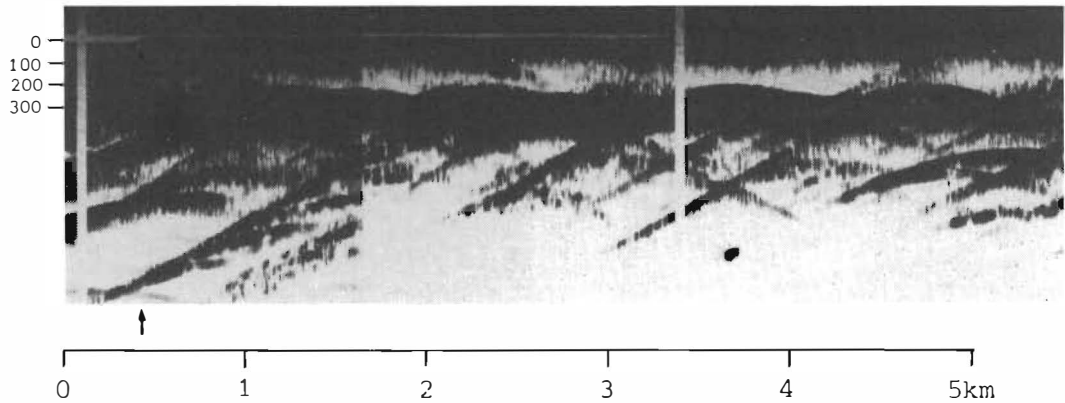


Fig. 14. Radio echo sounding 'Z' profile extending across the ice front (arrow) of Stancomb-Wills Ice Stream. Note hyperbolas from numerous bottom reflectors. Vertical exaggeration  $\approx 25\%$ .

## References

- Autenboer, T. van & Declair, H. 1972: Ice Thickness and Subglacial Relief of the Jelbartisen-Trolltunga Area, Dronning Maud Land. Pp. 713–722 in Adie, R.J. (ed.): *Antarctic Geology and Geophysics*. Universitetsforlaget, Oslo.
- Bentley, C.R., Clough, J.W., Jezek, K.C. & Shabtaie, S. 1979: Ice-thickness patterns and the dynamics of the Ross Ice Shelf, Antarctica. *Journal of Glaciology* 24, 287–294.
- Doake, C.S.M. 1976: Thermodynamics of the interaction between ice shelves and the sea. *Polar Record* 18, 37–41.
- Evans, S. & Smith, B.M.E. 1969: A radio echo equipment for depth sounding in polar ice sheets. *Journal of scientific instruments (Journal of Physics E) Ser. 2*(2), 131–136.
- Gow, A.J. & Rowland, R. 1965: On the relationship of snow accumulation to surface topography at 'Byrd station', Antarctica. *Journal of Glaciology* 5, 843–847.
- Gjessing, Y. 1984: Marine and non-marine contribution to the chemical composition of snow at Riiser-Larsenisen ice shelf in Antarctica. *Atmospheric environment* 18, 825–830.
- Gjessing, Y. & Wold, B. 1986: Absolute movements, mass balance and snow temperatures of Riiser-Larsenisen, Antarctica. *Nor. Polarinst. Skr.* 187, 23–31 (this volume).
- Jezek, K.C. & Bentley, C.R. 1983: Field studies of bottom crevasses in the Ross Ice Shelf, Antarctica. *Journal of Glaciology* 29, 118–126.
- Neal, C.S. 1979: The dynamics of the Ross Ice Shelf revealed by radio echo sounding. *Journal of Glaciology* 24, 295–307.
- Orheim, O. 1980: Physical characteristics and life expectancy of tabular Antarctic icebergs. *Annals of Glaciology* 1, 11–18.
- Orheim, O., Gjessing, Y., Lunde, T., Repp, K., Wold, B., Clausen, C., & Liestøl, O. 1986: Oxygen isotopes and accumulation rates at Riiser-Larsenisen, Antarctica. *Nor. Polarinst. Skr.* 187, 33–47 (this volume).
- Repp, K. 1978: Snow accumulation and snow stratigraphy on Riiser-Larsenisen, Dronning Maud Land, Antarctica. *Nor. Polarinst. Skr.* 169, 81–92.
- Robin, G. de Q. 1979: Formation, flow, and disintegration of ice shelves. *Journal of Glaciology* 24, 259–271.
- Smith, B.M.E. & Evans, S. 1972: Radio echo sounding: Absorption and scattering by water inclusions and ice lenses. *Journal of Glaciology* 11, 133–146.
- Swithinbank, C.W.M. 1957: Glaciology I. The morphology of the ice shelves of western Dronning Maud Land. *Norwegian-British-Swedish Antarctic Expedition, 1949–52, Scientific Results* 3A, 3–37.
- Thomas, R. H. 1973: The dynamics of the Brunt Ice Shelf, Coats Land, Antarctica. *British Antarctic Survey Scientific Reports* 79, 45 pp.
- Thomas, R.H. & MacAyeal, D.R. 1982: Derived characteristics of the Ross Ice Shelf, Antarctica. *Journal of Glaciology* 28, 397–412.

# Appendix

## SPRI radio echo sounding of Riiser-Larsenisen

*By David Drewry, Scott Polar Research Institute, Cambridge, England*

Part of Riiser-Larsenisen was sounded in January 1970 as part of a joint radio echo sounding programme between the Scott Polar Research Institute (SPRI), Cambridge and U.S. National Science Foundation.

SPRI Mk IV 60 MHz units with photographic recording were mounted in a US Navy C-130 F Hercules aircraft. Two terminated dipole antennae were mounted beneath the tail of the aircraft. Fixed bank angle tests indicated that the absolute power gain of the antennae was below specification, although the directional diagrams were excellent. This reduced performance affected penetration of deep plateau ice but not thinner ice in the vicinity of ice shelves and nunataks.

Navigation was by the use of SFIM flight recorder data tied to photographic and visual fixes of known surface features. In this area of Dronning Maud Land, however, no accurate surface maps were available in 1970, and this prevented the detailed plotting of flight tracks and the full reduction of data. In 1982 the flight was reconstructed using Landsat imagery, together with the Norsk Polarinstitutt maps of Vestfjella and ice front data from the NARE survey. It proved possible to fix the flight track on key points in Heimefrontfjella and Vestfjella, and on ice rises, grounding lines and crevasse fields. Between these points the aircraft position was interpolated by dead-reckoning based upon flight recorder data. The likely accuracy of the tracks away from a fix is considered to be in the order of 5–10 km at worst.

Ice thicknesses were digitized from the radar recorder and a sample is shown at approximately every 6 km (see Fig. 12 of preceding article). Their accuracy is approximately 10 m.

The SPRI radio echo sounding results in Riiser-Larsenisen display a pattern in which there is steady thickening inland from the ice front followed by a narrower zone of thinning

before major ice thickening again occurs at the grounding line. The absolute values of the ice thickness vary from line to line: the easternmost transect displaying the thinnest ice (maximum ice depth 250 m), those in the west the thickest (maximum ice depth 450 m). In the latter case the greater ice depths probably result from the effects of ice discharge from Veststraumen. The pattern, however, is not common. Further west on the Brunt ice shelf, for instance, Thomas (1973) reports an irregular but steady ice thickening from the ice front to the grounding line.

Just to the west of the NARE flight lines the SPRI flight track crosses the ice front over an area of grounding. A small ice rise occurs at the head of a complex inlet. The radio echo sounding records show a return typical of grounded ice and show an ice thickness of just over 400 m and quite comparable with that recorded over Kvitkuven to the east.

On the inland sections the radio echo sounding results are intermittent but depict a fairly rugged sub-glacial topography which represents the sub-ice extension of Heimefrontfjella. Ice thicknesses reach a maximum recorded value of 1850 m and typically range between 750 and 1300 m.

On the Stancombe-Wills Ice Tongue one line of radio echo sounding was undertaken (see Fig. 13 of preceding article). The flight track was well fixed from vertical aerial photographs tied to Landsat images. Numerous features on both the photos and the satellite image which relate to flow lines and crevasse patterns were easily identifiable and enabled the aircraft track to be located to closer than 200 m. Moving northwards from the front of the Brunt Ice Shelf the ice-water interface is relatively clearly defined on the radar records, but the pattern of reflections becomes complex as the western edge of the Stancombe-Wills Ice Tongue is encountered. In

this region the tongue does not have a clearly marked margin, being composed of a mosaic of disarticulated blocks, many up to several tens of kilometres in length. The blocks are connected by much thinner ice, possibly composed in large part of sea ice. The radio echo soundings show considerable scattering from this rough terrain with numerous hyperbolae generated from the exposed edges of the large ice blocks. Within the central and continuous zone of the ice tongue radar records display consistent returns with ice thicknesses between 300 and 450 m. The eastern boundary is clearly defined with a sharp break between returns, dominated by scattering with diffuse bottom echoes and typical ice shelf profiles with strong surface and bottom returns and little scattering. No pronounced ice thickness change occurs across the ice stream/ice shelf junction.

## Acknowledgements.

The radio echo sounding ice thickness measurements were conducted under UK NERC Research Grant GR3/420 and GR3/2291. Generous logistic support was provided by US NSF Office (now Division) of Polar Programs and US Navy. Fuel and facilities at Halley were generously provided by the British Antarctic Survey.

## Reference

Thomas, R. H. 1973: The dynamics of the Brunt Ice Shelf, Coats Land, Antarctica. *British Antarctic Survey Scientific Reports* 79. 45 pp.

# Absolute movements, mass balance and snow temperatures of the Riiser-Larsenisen Ice Shelf, Antarctica\*

Gjessing, Y. & Wold, B. 1986: Absolute movements, mass balance and snow temperatures of the Riiser-Larsenisen Ice Shelf, Antarctica. *Nor. Polarinst. Skr.* 187, 23–31.

Accumulation, deformation, absolute velocity, and snow temperatures at 10 m depth have been measured on Riiser-Larsenisen. Accumulation was measured at several points between the ice front and the grounding line, as well as on the top of an ice dome, for the period 1977–1979. Snow density varied from 470 kg/m<sup>3</sup> to 510 kg/m<sup>3</sup>, and the mean annual accumulation for twelve points on flat ice shelf was 608 kg m<sup>-2</sup>yr<sup>-1</sup>. At the top of the 200 m high dome the mean accumulation was only 416 kg m<sup>-2</sup>yr<sup>-1</sup>.

The velocities varied from 130 m.yr<sup>-1</sup> some 10 km from the grounding line to 110 m.yr<sup>-1</sup> near the ice front. By considering mass-continuity between two flow lines, the sum of bottom melting and disequilibrium was calculated for 7 locations across the shelf. Assuming steady state conditions, values of apparent melt rates were 900 kg m<sup>-2</sup>yr<sup>-1</sup> near the ice front and a maximum of 1700 kg m<sup>-2</sup>yr<sup>-1</sup> some 10 km from the grounding line. Thus, bottom melting is about 80% of the total 'ablation' if the ice shelf is in a steady state.

Snow temperatures at 10 m depth were measured on the ice shelf, on an ice dome, and at higher elevations inland. The temperature decreases from -16.8°C near the ice front to -19.2°C near the grounding line. At 695 m a.s.l. a few kilometres inland from the grounding line the temperature was -17.7°C, and on the ice dome it was -15.4°C and -16.4°C at 95 and 200 m a.s.l. respectively. These measurements indicate that the mean annual air temperatures, estimated from 10 m deep snow temperatures, apply only to a boundary layer immediately above the surface of the snow.

*Yngvar Gjessing, Geophysical Institute, University of Bergen, 5000 Bergen, Norway; Bjørn Wold, Norwegian Water Resources and Electricity Board, P.O.Box 5091, Majorstua, 0301 Oslo 3, Norway; November 1982 (revised August 1983).*

## Introduction

Riiser-Larsenisen is an ice shelf situated on the coast of Dronning Maud Land, Antarctica (Fig. 1). The work described in this paper was carried out during two Norwegian Antarctic Expeditions, one in 1976–77 and one in 1978–79. The field work was conducted in January–February 1977 and in February 1979.

The predominant wind direction in this area is from ENE, and typical summer temperatures range from 0° to -20°C.

Riiser-Larsenisen was studied briefly by Torbjørn Lunde (1961) during the 1958/59 Norwegian Expedition. At Maudheim, some 230 km to the east, extensive glaciological investigations were conducted during the Norwegian-British-

Swedish Antarctic Expedition 1949–52 (Schytt 1958; Swithinbank 1957). Further to the east, glaciological work was carried out by the Norwegian Expedition 1956–60, based at Norway Station (Lunde 1961).

The part of the ice shelf investigated is situated between 14° and 17° W and between 72° and 74° S. It extends 120 km from the coast to the Vestfjella mountains. Except for a few smaller areas the shelf is relatively flat and free from crevasses. Our base camp in 1977 – Camp Norway 3 – was situated some 3 km from the coast at 35 m a.s.l. About 15 km inland from the shelf edge, the gentle surface of the shelf was broken by a shallow depression 2.5 km wide and running ENE-WSW, which separated the peninsula of Camp Norway 3 from the rest of the shelf. Upon

\*Publication No. 50 of the Norwegian Antarctic Research Expedition 1976/79.

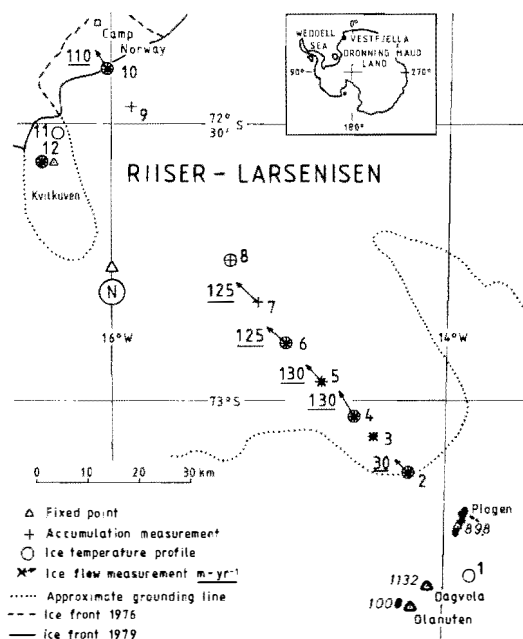


Fig. 1. Map of the area.

our return to the area in 1979 the peninsula had broken off along this depression. Some 30–40 km further inland, however, the surface was broken by transverse undulating valleys with a wavelength of approximately 5 km and an amplitude of about 10 m. Inland of this area and close to the grounding line, the shelf had a more irregular surface, with numerous hollows and crevasses. The elevation of the shelf increases inland to a maximum of 80 m a.s.l. about 10 km from the grounding line and then decreases to 60 m a.s.l. at the grounding line.

The most outstanding feature of the part of the ice shelf we studied is a prominent ice dome, Kvitkuven, situated on the outer part of the shelf some 20 km southeast of Camp Norway 3. This dome is 30 km long, and its summit reaches approximately 200 m a.s.l. Numerous relatively small crevasses surround it, indicating the presence of a 10 km wide shear zone between the dome and the floating ice moving around it.

### Field programme

In February 1977 three nets, each with six stakes, were laid out over three areas of about 4 km<sup>2</sup> as part of a combined absolute motion, strain rate,

and accumulation investigation. For a more detailed study of absolute movement and accumulation, 8 additional stations of two stakes each were established.

The positions of the stakes were determined by mutual observations, with a Wild T-2 theodolite, using the stake points, from the trigonometric station located inland from the grounding line and on the ice dome near the shelf edge. These measurements were all repeated in February 1979 except for those on the outermost stake net that had been partly broken off. The absolute motion, deformation, and mean accumulation were calculated. Snow densities were measured at 6 positions in 3–4 m deep snow pits.

Temperatures were measured at 10 m depths in eight boreholes. Thermistors and a wheatstone bridge were used for these measurements. The system was calibrated before and after the field work, and the accuracy of the measurements is probably within  $\pm 0.05^\circ\text{C}$ .

The height variations of the shelf surface along the stake line were determined by barometric levelling, which was repeated every time we crossed the shelf – six times in all. Local variations in air pressure were registered at the base camp, and the field measurements were corrected for these variations when the heights were calculated. The standard deviations for the six observations were approximately  $\pm 2$  m.

## Results and discussion

### Accumulation

Snow accumulation on Riiser-Larsenisen was measured at 21 points between the ice front and the grounding line for the period February 1977–February 1979. It was also measured at six points at the top of the ice dome Kvitkuven (Fig. 1). Aluminium stakes, 6 m long, were erected, and measurements taken during two weeks in January and February 1977. These were re-measured in February 1979. Five additional stakes that were placed in the shear zone between the ice shelf and the ice dome, could not be found in 1979 and had presumably been covered by snow. If that was the case, the snow accumulation on the shelf near the ice dome had been more than 350–400 cm during the period

1977–1979, or 50–60% higher than the accumulation elsewhere on the shelf at the same distance from the coast. Snow drift may account for this anomaly. Swithinbank (1957), for example, found that for the Maudheim Ice Shelf, even slight surface slopes resulted in abnormal accumulation values, but that the accumulation rates measured at various places on flat surfaces coincided within a few centimetres. It was also evident that the rate of accumulation increased with distance from the ice front. To obtain a representative accumulation value for the Maudheim Ice Shelf, Swithinbank had to exclude the stakes within 2 km of the coast. This agrees with our results. If we omit the stakes near the ice front, at the ice rise and near the grounding line, the mean snow depth at the other 12 stakes is 2.48 m,

and the standard deviation is 0.11 m. The measurements near the ice front and at the top of the ice rise showed less accumulation, probably due to snow loss from the area by drifting. The measurements near the grounding line gave variable results, due to drifting and the broken surface.

Densities in the upper 3 m were measured at seven points across the ice shelf. The density varied from 470 kg/m<sup>3</sup> to 510 kg/m<sup>3</sup>. The values are consistent with the mean density of 481 kg/m<sup>3</sup> in a 3.40 m deep pit near Maudheim, measured by Schytt (1958). Our lowest values were measured on the inner half of the shelf and at the top of Kvitkuvén (200 m a.s.l.). The highest values were at the grounding line and on the outer part of the shelf. Mass balance data are summarized in Table 1.

Table 1. Mass balance data from the Maudheim ice shelf.

Site	1	2	3	4	5	6	7	8	9	10	11	12
Distance from grounding line (km)	-30	0	10	15	25	35	45	55	95	105	100	100
Height above sea level, H (m)	695	60	80	76	65	59	55	54	45	35	95	200
Mean snow density Density 0–3 m (kg·m <sup>-3</sup> )		510		470		490		510		500		
Snow temperature 10 m depth (°C)	-17.7	-19.2		-18.4		-18.8		-18.6		-16.8		-16.4
Precipitation mean 1977–79 (kg·m <sup>-2</sup> yr <sup>-1</sup> )		583 <sup>A</sup>	584	579	639	591	639	613	593	598 <sup>A</sup>		416
Velocity U (horizontal) (m·yr <sup>-1</sup> )		31	130	125	125	120				110		
Total thickness calculated, H (m)		414	580	554	455	407	391	556	293	210		
Mean density $\bar{\rho}_1$ (kg·m <sup>-3</sup> )		884	893	892	887	883	880	878	872	852		
Strain rate $\dot{\epsilon}_z = -H \cdot \frac{\partial u}{\partial x} \cdot \bar{\rho}_{ice}$ (kg·m <sup>-2</sup> yr <sup>-1</sup> )		-3000 <sup>B</sup>	500	0	200	100				100		
Advective terms $u \cdot \frac{\partial H}{\partial x} \cdot \rho_{ice}$ (kg·m <sup>-2</sup> yr <sup>-1</sup> )		500	-600	-1100	-500	-400				-200		
Sum bottom melt disequilibrium (kg·m <sup>-2</sup> yr <sup>-1</sup> )		-2900	1700	1700	1300	1100				900		

A: Mean of 6 stakes

B: Direct measurement ( $\epsilon_x + \epsilon_y$ )

Bentley et al. (1964) published a map of the mean density in the upper 2 m of snow in Antarctica. According to this map, the shelf area in Dronning Maud Land had densities higher than  $450 \text{ kg/m}^3$ . These were among the highest densities measured for the upper 2 m of snow in Antarctica, and except for the shelf area in Dronning Maud Land they occur very rarely. On the Filchner Ice Shelf further south and west the density values are between 350 and  $390 \text{ kg/m}^3$ .

The water equivalent of the snow pack was calculated for all measured stakes. For points without density measurements we have interpolated linearly between the nearest measurements. In terms of water equivalent the accumulation on the flat shelf is quite uniform. The mean water equivalent for the previously mentioned twelve points (Fig. 1) across the shelf is  $610 \text{ kg m}^{-2}\text{yr}^{-1}$ , and the standard deviation is  $30 \text{ kg m}^{-2}\text{yr}^{-1}$ . For the six measured points at the top of the Kvitkuven ice rise (200 m a.s.l.) the mean water equivalent is  $420 \text{ kg m}^{-2}\text{yr}^{-1}$ .

Swithinbank (1957) concluded that because of the large extent of the level ice shelf in the direction of the prevailing winds, drifting snow cannot cause a net change in surface level. This implies that, in the absence of net melting or appreciable evaporation, the accumulation rate will give a satisfactory measure of precipitation. In a discussion of the origin of the accumulation, Swithinbank (1957) concluded that the bulk of the accumulation is a result of strong cyclonic winds from the north-east and east; drifting snow from the interior therefore does not affect accumulation.

During the NARE 1976–77 expedition, accumulation was studied in pits in the same area on Riiser-Larsenisen (Repp 1978). For 1976 Repp found values about 10–15% higher than the mean for the period 1977–79. On the other hand, values for 1975 were lower than the 1977–79 mean.

According to Schytt (1958), a normal annual layer in pits at Maudheim consists of a coarse grained, highly metamorphosed summer surface on top of a firn layer of varying grain size and ice content. This firn layer is coarse and has an abundance of ice pellets and ice layers in its upper part, showing that some melting takes place during a normal summer. This melting, however, is not sufficient to soak the entire annu-

al deposit. The same criteria were used to recognize the annual layers in the pits in 1977. In 1979 we also tried to find annual layers in the pits, in order to give the exact accumulation for each of the previous two years. This turned out to be a very difficult task, and in some places we did not even succeed in finding the summer surface of 1977. These poorly developed summer surfaces may be due to cold and/or relatively snowy summers.

Our figures from the period 1977–79 give much higher values than previous measurements from ice shelf areas in Dronning Maud Land. At Maudheim the mean accumulation between 1935 and 1951 was  $365 \text{ kg m}^{-2}\text{yr}^{-1}$  (Schytt 1958), and  $420 \text{ kg m}^{-2}\text{yr}^{-1}$  for 1952 to 1960 (Swithinbank 1962). At Norway Station the mean accumulation was  $484 \text{ kg m}^{-2}\text{yr}^{-1}$  for the period 1950–59 (Lunde 1961). Whether our higher accumulation values are due to a generally higher precipitation at Riiser-Larsenisen, a change of climate, or simply casual variations, is discussed by Orheim et al. (1986, this volume), based on  $\text{O}^{18}/\text{O}^{16}$  isotope studies on ice cores that we brought home. It should be mentioned, however, that the mean accumulation in Halley for the years 1975–79 is  $535 \text{ kg m}^{-2}\text{yr}^{-1}$ , which is 145% of the mean accumulation for the preceding 18 years.

### *Absolute motion and deformation*

The sites 2–6 (Fig. 1) were marked with  $3 \text{ m}^2$  flags of black canvas stretched between two poles. The positions of these sites were determined by theodolite observations from these points and from four trigonometric stations on bedrock. After repeating the observations two years later, the absolute motion was determined. By independent calculations of the movements based on different trigonometric points, the accuracy of the calculations was found to be  $\pm 2\text{--}5\%$ .

The absolute motion of site 10 near the ice front was determined by observations from site 10 and from a base line at site 12 on the top of Kvitkuven. Observations of a stake pattern that was set out on Kvitkuven gave mean horizontal strain rates ( $\dot{\epsilon}$ ) averaged over two years of  $8\text{--}17 \cdot 10^{-4} \text{ year}^{-1}$  and a clockwise rotation relative to the trigonometric station inland of  $0.015^\circ$

yr<sup>-1</sup>. By compensating for this rotation the calculated movement of site 10 is probably accurate to within ±5%.

The results given in Table 1 show that the absolute motion of 31 m year<sup>-1</sup> near the grounding line increases to 130 m year<sup>-1</sup> 10 km downstream. Further downstream the velocities decrease to 110 m year<sup>-1</sup> near the ice front.

For comparison these velocities are about 30% of those on the Brunt Ice Shelf (Limbirt 1964).

### Mass balance

The equilibrium of an ice shelf can be assessed by considering mass-continuity as the ice shelf passes between two flowlines in the x direction, thus:

$$(1) \quad \frac{D}{Dt} \bar{\rho}_i \dot{H} = \dot{A} - \dot{M} + \bar{\rho}_i \dot{\epsilon}_z = \frac{\partial}{\partial t} \bar{\rho}_i H + u \frac{\partial}{\partial x} \bar{\rho}_i H$$

where x is the distance along the flow line, H is the ice thickness,  $\frac{\partial}{\partial t} \bar{\rho}_i H$  is the rate of thickening of the ice sheet,  $\frac{\partial}{\partial x} \bar{\rho}_i H$  is the thickness gradient along the flow line,  $\dot{\epsilon}_z$  is the vertical strain rate and is negative for thinning,  $\dot{M}$  is the bottom melting rate,  $\dot{A}$  is the snow accumulation rate, and  $\bar{\rho}_i$  is the mean ice density. The absolute motion, u, is assumed to be independent of depth, which is probably valid where the shelf is floating.

Where the ice is floating the total ice-thickness can be expressed as:

$$(2) \quad H = h \cdot B$$

where h is height above sea level of the surface and

$$(2a) \quad B = \frac{1}{1 - \bar{\rho}_i / \bar{\rho}_w}$$

where  $\bar{\rho}_i$  and  $\bar{\rho}_w$  are the mean densities of ice and sea water respectively. This expression is derived from consideration of the buoyancy of the ice, thus:

$$(3) \quad - \int_0^H \rho_w \cdot dz = - \int_0^h \rho_i \cdot dz$$

where z = 0 is the sea level,

$$\text{or} \quad \bar{\rho}_w (H-h) = \bar{\rho}_i \cdot H$$

so

$$(3) \quad H = h \cdot \frac{1}{1 - \bar{\rho}_i / \bar{\rho}_w} = h \cdot B$$

Densities of ice shelves have been studied in a number of boreholes. Schytt (1958) found a mean density of 852 kg m<sup>-3</sup> for the upper 200 m of the ice shelf near Maudheim – about 200 km from Riiser-Larsenisen. If ice deeper than 200 m has a uniform density of 915 kg m<sup>-3</sup>, the mean density for a 400 m thick ice shelf will increase to about 885 kg m<sup>-3</sup>.

Based on these results the mean ice density  $\bar{\rho}_i(H)$  can be expressed as;

$$(4) \quad \bar{\rho}_i(H) = \frac{1}{H} (200 \cdot 852 + (H-200) \cdot 915) = 915 - \frac{12600}{H}$$

Combining (2a) and (4) we find that B is about 7.5 for the thickest parts of the shelf and 5.8 near the ice front.

The glaciological programme of NARE 1978–79 also included radio echo soundings from helicopters (Orheim 1983). The average thickness of the ice shelf based on his results (Fig. 2), increased from approximately 230 m near the ice front to more than 650 m near the grounding line. Our values, calculated from equation 4, varied from 210 m near the ice front to 580 m about 10 km from the grounding line and then decreased to 515 m in the depression near the grounding line. In addition, as noted, a number of undulations of the shelf surface of some 5 km in length and 5–10 km amplitude were observed.

As navigational uncertainties were 0.5–5 km for the radio echo flights, and because the flight lines mostly deviated from our stake line, the calculation of  $\frac{\partial H}{\partial x}$  based on altimeter levelling gives the most accurate data for the stake lines.

We assume the ice to be incompressible,  $\dot{\epsilon}_z = -(\dot{\epsilon}_x + \dot{\epsilon}_y)$ . Transverse strain is found to be very small for floating ice shelves. Arduis (1964) and Limbirt (1964) measured transverse strain rates of 0–7 · 10<sup>-4</sup> year<sup>-1</sup> on the Brunt Ice Shelf. For comparison the strain rate parallel to the flow,  $\frac{\partial u}{\partial x}$ , was of order of magnitude 10<sup>-3</sup> yr<sup>-1</sup> on Riiser-Larsenisen.

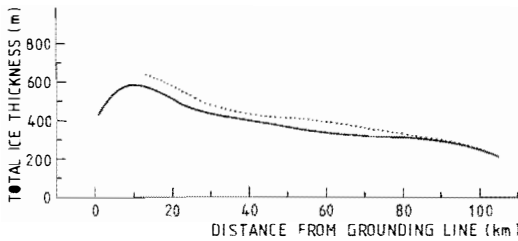


Fig. 2. Profile of total ice thickness of the Riiser-Larsen Ice Shelf based on barometric levelling along the stake line (full drawn line) and radio echo soundings from helicopter (dotted line).

Direct measurements of  $\dot{\epsilon}_x$  and  $\dot{\epsilon}_y$  were carried out near the grounding line and gave values of  $\dot{\epsilon}_x$  and  $\dot{\epsilon}_y$  of  $5.3 \cdot 10^{-2}$  and  $2.5 \cdot 10^{-2} \text{ year}^{-1}$  respectively. This area is affected by diverging streams from inland. It also serves as a hinge between the floating part of the shelf that is affected by tides and the grounded part. This explains the high strain rate in this area.

As seen from Fig. 1 the deviations between the flow line and the stake line were less than  $5^\circ$  for the inner parts of the stake line. Therefore, with good approximation eq. 1 can be solved to give the sum of bottom melting  $\dot{M}$  and disequilibrium  $\bar{\rho}_1 \frac{\partial H}{\partial t}$  for seven stations at different distances from the grounding line. The accuracy of these calculations is, however, sensitive to the value of  $\frac{d}{dx} \bar{\rho}_1 H$ .

The standard deviation of six independent observations of height differences between adjacent stakes was approximately  $\pm 2$  m. This corresponds to an accuracy of our determination of  $\frac{\partial H}{\partial x}$  of about 10% for the steepest slopes to some 50% for gentler slopes. The values of  $u$  and  $\dot{A}$  are within 5%. This corresponds to an accuracy of  $\pm 30 \text{ kg} \cdot \text{m}^{-2} \text{ yr}^{-1}$  for  $\dot{A}$ ,  $100\text{--}200 \text{ kg} \cdot \text{m}^{-2} \text{ yr}^{-1}$  for the term  $u \cdot \frac{\partial}{\partial x} \bar{\rho}_1 \cdot H$ , and an accuracy of  $50 \text{ kg} \cdot \text{m}^{-2} \text{ yr}^{-1}$  for the determination of  $H \cdot \bar{\rho}_1 \cdot \frac{du}{dx}$ .

In eq. 1  $\frac{\partial H}{\partial x}$  is the gradient in the flow direction. At St. 10 near the ice front, only the velocity component perpendicular to the ice front was determined. However, here very low values of  $\frac{dH}{dx}$  were found, so that the error introduced by any deviation between the direction of  $u$  and the velocity component perpendicular to the ice front leads to only small errors in  $u \cdot \frac{\partial H}{\partial x}$ . Conse-

quently, the uncertainty in the determination of the sum of bottom melting and disequilibrium of the shelf should be within  $\pm 300 \text{ kg} \cdot \text{m}^{-2} \text{ yr}^{-1}$  for site 2 and about  $\pm 200 \text{ kg} \cdot \text{m}^{-2} \text{ yr}^{-1}$  for the remaining sites.

The results of these calculations are given in Table 1. Near the grounding line, strain rate measurements showed that the contribution from vertical strain rate  ${}_i H \dot{\epsilon}_z$  was  $-3.0 \cdot 10^3 \text{ kg} \cdot \text{m}^{-2} \text{ yr}^{-1}$  leading to a value of  $-2.9 \cdot 10^3 \text{ kg} \cdot \text{m}^{-2} \text{ yr}^{-1}$  for the sum of bottom melting and disequilibrium. In this area the shelf is probably partly grounded and partly floating so that the theory leading to eq. 2 does not strictly apply. However, in this area cold ice masses from inland coming into contact with sea water could freeze a considerable volume of sea water at the base of the ice shelf before the ice temperature profile is adjusted to new steady state conditions. This area also serves as a hinge between the floating part of the ice shelf, affected by tides, and the grounded part. Bottom crevasses resulting from such tidal action may become filled with sea water that will freeze, except for a volume of brine that is enclosed in the crevasses.

About 10 km downstream from the grounding line the sum of disequilibrium and bottom melting has increased to a positive value of  $1700 \text{ kg} \cdot \text{m}^{-2} \text{ yr}^{-1}$ . Further downstream it decreases and is found to be  $900 \text{ kg} \cdot \text{m}^{-2} \text{ yr}^{-1}$  near the ice front. In these areas we have assumed zero lateral strain, so that  $\dot{\epsilon}_z = -\frac{\partial u}{\partial x}$ . This assumption is probably valid near the ice front, but further upstream there may be an effect of lateral compression due to converging ice streams. This would tend to make estimates of  $\dot{M} + \frac{\partial}{\partial t} \rho H$  too high.

The rate of accumulation is an average for the two periods, 1977–79. Studies of  $\text{O}^{18}\text{--O}^{16}$  ratios of snow samples collected down to 10–13 m at 2 locations in this area (Orheim et al. 1986) indicate that the 1977–79 accumulation was approximately 60% higher than the mean values of the 15 year period. When this 15 year mean accumulation value of  $350 \text{ kg} \cdot \text{m}^{-2} \text{ yr}^{-1}$  is introduced, the sum of bottom melting and disequilibrium will be reduced by a  $150\text{--}200 \text{ kg} \cdot \text{m}^{-2} \text{ yr}^{-1}$ .

Most papers in which estimation of melting and freezing rates under ice shelves are made (Table 2), assume a steady state,  $\frac{\partial H}{\partial t} = 0$ , and find that bottom melting decreases with distance

Table 2. Rates of bottom melting (sum of bottom melting and disequilibrium) from other areas.

Site	Bottom melting $\text{Mg} \cdot \text{m}^{-2} \cdot \text{yr}^{-1}$	Reference
Brunt ice shelf (near ice front)	0.376	Limbert 1964
Brunt ice shelf (near ice front)	0.20–0.25	Ardus 1964
Brunt ice shelf (near ice front)	1–3	Thomas 1973
Maudheim (ice front)	0.9	Swithinbank 1957
Ross Ice shelf (ice front)	0.6	Crary 1964
Ross Ice shelf (near Ross Island)	1.3	Paige 1969
Ross ice shelf	0–0.70	Crary et al. 1962
Ross ice shelf (near Ross Island)	0.9	Thomas & Bentley 1978
Filchner ice shelf (ice front)	9.5	Behrendt 1962
George VI ice shelf	1–8	Bishop & Walton 1981

from the ice front. If we assume a steady state, we find a small increase in the rate of bottom melting with distance upstream, which could be used as an argument for rejection of the steady state assumption. On the other hand, the water at the ice-water interface must be at the pressure melting point for that depth and for ice or water salinity,  $T_m(S,P)$ . The important question is how fast heat can be transferred through this boundary layer. This depends on currents under the ice shelf, the stability and temperature of the water masses under the shelf, which may change as ice melts or forms, and the temperature gradient in the ice. Ice is a poor conductor of heat. McAyeal (1983) found by theoretical considerations that the basal melting removes the warmest part of the ice column faster than the temperature-depth profile can adjust by conduction. The heat transfer is proportional to the difference between the water temperature  $T_w$  and  $T_m(S,P)$ .

The effect of pressure on melting temperature can be expressed as

$$(5) T_m(S,P) = T_m(S,O) - 0.00759 p$$

(Fujino et al. 1974) where  $p$  is the pressure in bars measured above atmospheric. This leads to a decrease in  $T_m$  of 0.15–0.20°C under the thickest parts of the shelf compared to the ice front. Under the thickest parts of the shelf there is a 'salty' ice layer that was formed by freezing near the grounding line. This also leads to a decrease in  $T_m$ . Under this part of the shelf the difference  $T_w - T_m$ , therefore, has its maximum. Further downstream the 'salty' ice layer has been removed by melting, leading to an increase of  $T_m$ . The

warmest water in the sub-ice shelf cavity resides at the sea bed because of its high salinity. McAyeal (1983) found by theoretical considerations that turbulence generated by tidal currents is sufficiently strong to completely mix the water column against buoyancy input for water layer thickness less than about 100 m. The rate of melting under the ice shelf therefore depends on bottom topography, which is unknown at Riiser-Larsenisen.

Table 2 shows some calculated values of bottom melting from other areas in Antarctica. Most of these calculations have been made assuming a steady state, and only a few studies have been carried out to check this assumption. For example, by re-leveling after an interval of three years Coslett et al. (1975) found no significant changes in surface profiles of the Brunt Ice Shelf, thus suggesting that a steady state existed here. In contrast, Thomas & Bentley (1978) found a local ice thickening with an average value of 0.34 m of ice per year near the southeastern corner of the Ross Shelf.

The sum of bottom melting and disequilibrium near the ice front on Riiser-Larsenisen of  $900 \text{ kg m}^{-2} \cdot \text{yr}^{-1}$  is the same as Swithinbank found for the ice front near Maudheim (Table 2), while the values for the Brunt Ice Shelf and the Filchner Ice Shelf are higher by a factor of about 3 and 9 respectively. The maximum melting rates under the George VI Ice Shelf (Bishop & Walton 1981) are higher than on Riiser-Larsenisen by a factor of 5, and the maximum melting rates occur in the area of maximum ice thickness.

According to Carmach & Foster (1975), the

westward moving Antarctic coastal current enters the Southern Weddell Sea as a concentrated flow of about  $0.5 \text{ m s}^{-1}$  following the contours of the continental margin. Near  $27^\circ \text{W}$ , divergence occurs, and most of the current leaves the coast. This may explain the comparatively high rates of bottom melting under Riiser-Larsen compared to the Brunt Ice Shelf.

If we assume a linear variation between the points of observation for the parameters in eq. 1, the following rough estimate of the mass budget for a section of 1 m width from the ice shelf to the grounding line is obtained:

Precipitation	+ 63	$10^3 \text{ ton m}^{-1}\text{yr}^{-1}$
Sum bottom melting and disequilibrium	— 98	»
Calving	— 17	»
<hr/>		
Residual	— 52	$10^3 \text{ ton m}^{-1}\text{yr}^{-1}$

If the shelf is in a steady state, the residual of  $52 \cdot 10^3 \text{ ton} \cdot \text{m}^{-1}\text{yr}^{-1}$  would have to be supplied by flow from inland. This value is difficult to estimate as errors are introduced in the determination of bottom melting, precipitation, and calving, and in the steady state assumption.

The precipitation on the inland of Antarctica is primarily drained by a number of outlet glaciers. The mass transport through a 1 m wide section of these outlet glaciers is in the order of magnitude  $10^5 - 10^6 \text{ ton} \cdot \text{yr}^{-1}$  (Young 1979; Gjessing 1972). For the sector between longitudes  $80^\circ \text{E}$  and  $135^\circ \text{E}$ , Young (1979) found a total transport of about  $150 \cdot 10^9 \text{ ton yr}^{-1}$  from the inland to the coast, or about  $50 \cdot 10^3 \text{ ton m}^{-1}\text{yr}^{-1}$ , which is close to the value we found for the Riiser-Larsen Ice Shelf, using a steady state model. Budd et al. (1971) estimated the transport for larger areas of Antarctica to be in the range  $50-100 \cdot 10^3 \text{ ton m}^{-1}\text{yr}^{-1}$ .

### Snow temperatures

Snow temperatures at 10 m depths were determined by measurements in boreholes at eight locations (Fig. 1). For sixteen locations in Greenland and Antarctica, Loewe (1970) found a clear correspondence between snow temperatures at 10 m depth and mean annual screen temperatures 2 m above the snow surface. For six locations

in Antarctica in the elevation interval 30–1500 m the difference between the mean annual screen temperature and the snow temperature at 10 m depth ranges from  $+0.8-1.1^\circ \text{C}$ . The 10 m snow temperatures that we measured,  $T_a$  (Table 1), ranged from  $-16.8^\circ \text{C}$  near the ice front to  $-19.2^\circ \text{C}$  near the grounding line. Inland from the grounding line, at site 1,695 m a.s.l., the 10 m depth temperature increased to  $-17.7^\circ \text{C}$ , and at sites 11 and 12, on Kvitkuven 95 and 200 m a.s.l. respectively, it was  $-15.4^\circ \text{C}$  and  $-16.4^\circ \text{C}$ . This suggests mean temperature lapse rates of  $+0.35^\circ \text{C}$  per 100 m for a 640 m layer near the grounding line, and  $+0.24^\circ \text{C}$  per 100 m for a 165 m layer near the shelf edge. Near the shelf edge, however, the lapse rate is  $+2.8^\circ \text{C}$  per 100 m in the lowest 40 m layer, and in the next 100 m layer  $-1^\circ \text{C}$  per 100 m. The latter is close to the dry adiabatic lapse rate ( $0.98^\circ \text{C}/100 \text{ m}$ ). Liljequist (1957) found that at Maudheim, situated 5 km from the coast line, the annual mean height of the surface inversion was 495 m a.s.l. and the mean temperature gradient in this layer was  $1.2^\circ \text{C}$  per 100 m. For the layer from 2.5 to 10 m above surface level he found a mean annual difference of  $+1.8^\circ \text{C}$ . We may assume that the mean height of the inversion and the temperature lapse rate at Riiser-Larsen will not differ drastically from those in the Maudheim area. Sites 1 and 12 situated on vast horizontal snow fields, and to some extent site 11 situated on the  $2^\circ$  slope up to the ice dome, are affected by local ground inversions. This leads to lower mean air temperatures compared to the free atmosphere. Thus, the mean annual air temperatures estimated from snow temperatures at 10 m in depth apply only for a boundary layer immediately above the snow surface, and they are lower than the mean annual temperature would be at the same elevation in the free atmosphere.

### Acknowledgements

Thanks are extended to the members of the field party in 1977–78, led by T. Vinje, and to the leader of the expedition, O. Orheim. We also want to thank Dr. R. Hooke and Dr. B. Hallet for valuable criticism and for carefully reading the manuscript.

## References

- Ardus, D.A. 1964: Surface deformation. Absolute movement and mass balance of the Brunt Ice Shelf near Halley Bay. *British Antarctic Survey Bulletin* 4, 21–40.
- Behrendt, I.C. 1962: Geophysical and Glaciological Studies in the Filchner Ice Shelf area of Antarctica. *Journal of Geophysical Research* 67, (1), 221–234.
- Bentley, C.R., Cameron, R.L., Bull C., Kojima, K. & Gow, A.J. 1964: Physical Characteristics of the Antarctic Ice Sheet. *Antarctic Map Folio Series. Folio 2*. American Geographical Soc.
- Bishop, J.F. & Walton, J.L.W. 1981: Bottom melting under George VI Ice Shelf, Antarctica. *Journal of Glaciology* 27, (97), 429–447.
- Budd, W.F., Jenssen, D. & Radok, V. 1971: Derived physical characteristics of the Antarctic ice sheet. *ANARE Interim Reports Ser. A (IV) Glaciology* 120.
- Carmach, E.C. & Foster, T.D. 1975: Circulation and distribution of oceanographic properties near the Filchner Ice Shelf. *Deep Sea Research* 75, 77–90.
- Coslett, P.H., Guyatt, M. & Thomas, R.H. 1975: Optical levelling across an Antarctic ice shelf. *British Antarctic Survey Bulletin* 40, 55–63.
- Crary, A.P., Robinson, E.S., Bennet, H.F. & Boyd, W.W. 1962: Glaciological Regime of the Ross Ice Shelf. *Journal of Geophysical Res.* 67 (7), 2791–2807.
- Crary, A.P. 1964: Melting at the ice-water interface, 'Little America' station. *Journal of Glaciology* 5 (37), 129–30.
- Fujino, K., Lewis, E.L. & Perkin, R.G. 1974: The freezing Point of Seawater at Pressure up to 100 Bars. *Journal of Geophysical Res.* 79 (12), 1791–1797.
- Gjessing, Y. 1972: Mass transport of Jutulstraumen Ice Stream in Dronning Maud Land. *Norsk Polarinstittut Arbok* 1970, 227–232.
- Liljequist, G.H. 1957: Energy exchange of an Antarctic snow field. Part. 1. *Norwegian-British-Swedish Antarctic Exp. 1949–52. Scientific results* 2.
- Limbert, D.W.S. 1964: The absolute and relative movement and regime of the Brunt Ice Shelf near Halley Bay. *British Antarctic Survey Bulletin* 3, 1–11.
- Loewe, F. 1970: Screen temperatures and 10 m snow temperatures. *Journal of Glaciology* 9 (56), 263–268.
- Lunde, T. 1961: On the snow accumulation in Dronning Maud Land. Den Norske Antarktisekspedisjon 1956–60. Scientific Results I. *Norsk Polarinstittut Skrifter* 123.
- McAyeal, D.R. 1983: *Rectified tidal currents and tidal-mixing fronts: Controls on the Ross Ice Shelf flow and mass balance*. Ph.D. dissertation, Princeton University.
- Orheim, O. 1986: Radio echo sounding of Riiser-Larsenisen. *Norsk Polarinstittut Skrifter* 187, 5–22 (this volume).
- Orheim, O., Gjessing, Y., Lunde, T., Repp, K., Wold, B., Clausen, H. & Liestøl, O. 1986: Oxygen isotopes and accumulation rates at Riiser-Larsenisen. *Norsk Polarinstittut Skrifter* 187, 33–47 (this volume).
- Paige, R.A. 1969: Bottom melting of the McMurdo Ice Shelf, Antarctica, *Journal of Glaciology* 8 (52), 170–71.
- Repp, K. 1978: Snow accumulation and snow stratigraphy on Riiser-Larsenisen, Dronning Maud Land, Antarctica. Results from Norwegian Antarctic Research 1974–77. *Norsk Polarinstittut Skrifter* 169.
- Schytt, V. 1958: Glaciology. Snow studies at Maudheim. *Norwegian-British-Swedish Antarctic Expedition 1949–52. Scientific Results IV*.
- Swithinbank, C. 1957: Glaciology. The Regime of the Ice Shelves at Maudheim as shown by Stake Measurements. *Norwegian-British-Swedish Antarctic Expedition 1949–52. Scientific Results III*.
- Swithinbank, C. 1962: Maudheim revisited: The Morphology and regime of the Ice Shelf, 1950–60. *Norsk Polarinstittut Arbok* 1960.
- Thomas, R. H. 1973: The dynamics of the Brunt Ice Shelf, Coats Land, Antarctica. *British Antarctic Survey. Scientific Reports* 79, 1–45.
- Thomas, R.H. & Bentley, C.R. 1978: The equilibrium state of the eastern half of the Ross Ice Shelf. *Journal of Glaciology* 20 (84), 509–518.
- Thomas, R.H. & Coslett, P.H. 1970: Bottom melting of Ice Shelves and the Mass Balance of Antarctica. *Nature* 228, 47–49.
- Young, N.W. 1979: Measured velocities of interior East Antarctica and the state of mass balance within the I.A.G.P. area. *Journal of Glaciology* 24 (90), 77–88.



## Oxygen isotopes and accumulation rates at Riiser-Larsenisen, Antarctica\*

Orheim, O., Gjessing, Y., Lunde, T., Repp, K., Wold, B., Clausen, H. B. & Liestøl, O. 1986: Oxygen isotopes and accumulation rates at Riiser-Larsenisen, Antarctica. *Nor. Polarinst. Skr.* 187, 33–47.

Measurements of  $\delta^{18}\text{O}$  and  $\beta$ -activity on eight cores covering up to 20 years of precipitation show that the mean multi-year mass balance at Riiser-Larsenisen is 0.32 m water equivalent ( $320 \text{ kg m}^{-3}$ ). The Kvitkuven ice rise shows the smallest accumulation rates and inter-annual variability. There are no significant correlations in year-to-year variations in accumulation between the eight cores, or between the results at Riiser-Larsenisen and the records at the 'near-by' stations Halley and SANAE/Norway Station. Mean annual accumulations at these coastal stations and Maudheim Station and the mean from near the ice edge of Riiser-Larsenisen are identical within 5%, except for Norway station during the IGY period, which is 30% higher. Stake measurements during 1977–79 show higher accumulation rates than the long-term means determined by the isotopic measurements.

The mean  $\delta^{18}\text{O}$  variations correlate closely with mean annual temperatures, with a relationship  $= 1.3\text{‰}/^\circ\text{C}$ . This agrees well with results from the Antarctic Peninsula. Mean annual temperatures and mean  $\delta$  for all sites at Riiser-Larsenisen are  $-17.2^\circ\text{C}$  and  $-20.2\text{‰}$  respectively. Temperature observations and monthly measurements of  $\delta$ -concentrations in precipitation at Halley show that the conditions there are similar to those of Riiser-Larsenisen, with means for different periods of  $\sim 18.3^\circ\text{C}$  and  $-19.7\text{‰}$  respectively. However, the precipitation data show higher variability in  $\delta^{18}\text{O}$  than the snow/firn sections.

*Olav Orheim and Olav Liestøl, Norsk Polarinstitutt, P.O. Box 158, 1330 Oslo Lufthavn, Norway; Yngvar Gjessing, Geofysisk Institutt, Avd. B, 5014 Bergen Universitet, Norway; Torbjørn Lunde, 4500 Mandal, Norway; Kjell Repp, Norconsult A/S, Kjørbov. 20, 1300 Sandvika, Norway; Bjørn Wold, NYE, P.O. Box 5091, Majorstua, 0301 Oslo 3, Norway; Henrik B. Clausen, Geophysical Isotope Laboratory, København Universitet, Haraldsgade 6, 2200 København, Denmark.*

Riiser-Larsenisen is an ice shelf located between  $12^\circ\text{W}$  and  $20^\circ\text{W}$  in western Dronning Maud Land (Fig. 1). We report here mainly the results of isotope studies on ice samples collected from seven localities at Riiser-Larsenisen and one locality upstream from the ice shelf (Fig. 2). The programme was organized by Olav Liestøl and, later, by Olav Orheim, and the field work was done on three expeditions: Torbjørn Lunde collected samples from two locations on the Norwegian Antarctic Expedition 1968/69, Yngvar Gjessing, Kjell Repp and Bjørn Wold collected samples at five sites on the Norwegian Antarctic Research Expedition (NARE) 1976/77, and Gjessing and Wold collected one core on NARE 1978/79. Also included are results from two samples collected by Wold at Fimbulisen (Fig. 1) in 1978/79.

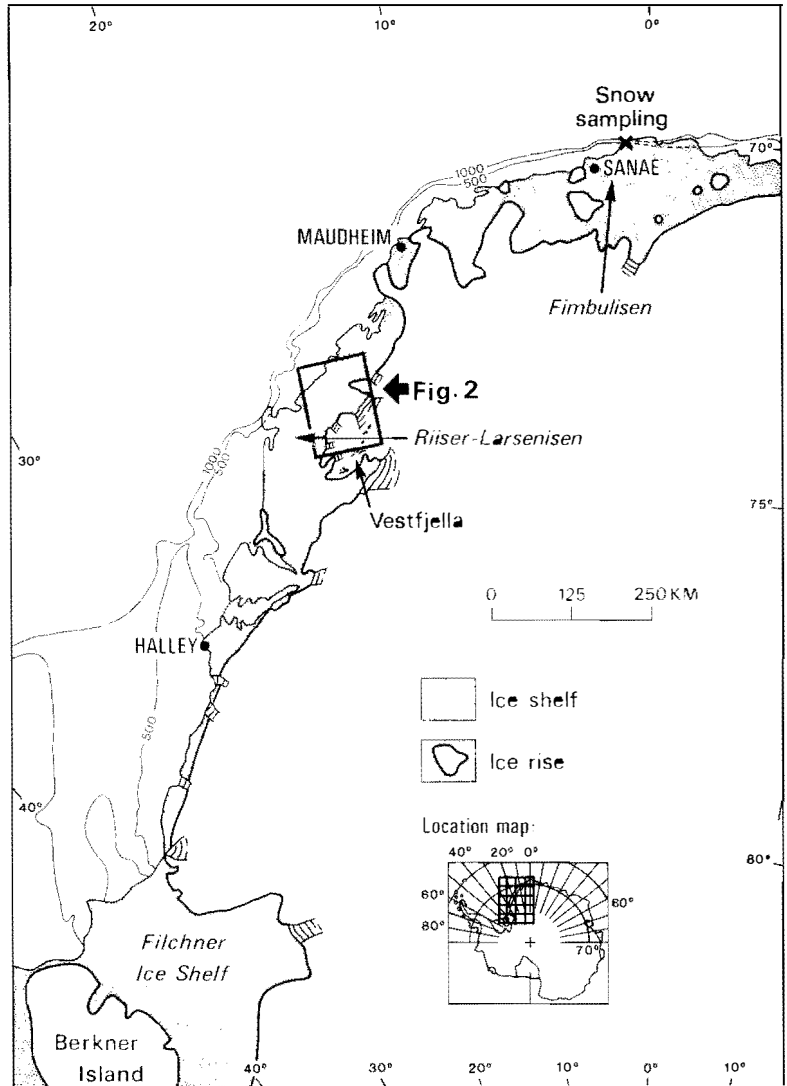
The 1968/69 samples were collected in connection with traditional pit studies and showed well-developed seasonal  $\delta^{18}\text{O}$  variations. It was

therefore decided to collect further samples for such analysis on NARE 1976/77 and 1978/79. Other glaciological studies on these two expeditions covered snow accumulation, temperatures, and chemistry, and ice flow and ice thickness. These are reported in Repp (1978), Gjessing (1984), Gjessing & Wold (1986), and Orheim (1986).

Samples were generally collected at 0.05 m intervals, following standard procedures. Either the samples were collected from the walls of snow pits, melted, and shipped in plastic bottles, (sampling sites 1,2,3,6,8), or they were collected as cores and kept frozen on shipment to Norway and subsequently to Denmark (sampling sites 4,5,7, and Fimbulisen). The isotope analyses were done at the Geophysical Isotope Laboratory, University of Copenhagen. All samples were analyzed for the concentration of  $\text{H}_2^{18}\text{O}$ , expressed as a relative difference ( $\delta^{18}\text{O}$ ) with respect to Standard Mean Ocean Water (SMOW) (e.g.

\* Publication No. 54 of the Norwegian Antarctic Research Expeditions (1976/77, 1978/79).

Fig. 1. Index map of studied areas, including sampling locality on Fimbulisen.



Craig 1961). Five of the sections were also analyzed for total  $\beta$ -activity. Fig. 1 shows the location of all sample sites, and Table 1 gives the time of collection, length of core, approximate number of years covered, and the depth of stratigraphic studies at each locality.

## Results

### *The isotope-measurements*

The measured variations in  $\delta^{18}\text{O}$  and in  $\beta$ -activity are shown in Figs. 3–10. Most sections show marked peaks in  $\beta$ -activity, which have been as-

signed to the 1964/65 and 1970/71 seasons, based on results from elsewhere in Antarctica (Picciotto et al. 1971; Clausen & Dansgaard 1977). The  $\beta$ -results indicate that at most one section, No. 5, extended as far back as 1955, when the total  $\beta$ -activity was built up in Antarctic snow (Picciotto & Wilgain 1963). The  $\delta^{18}\text{O}$  seasonal variations are generally well developed and differ in this respect from many other areas of Antarctica, e.g. Dansgaard et al. (1973). Thus, taken in conjunction with the gross activity, they allow reasonably confident identification of annual layers through most of the sampled depths.

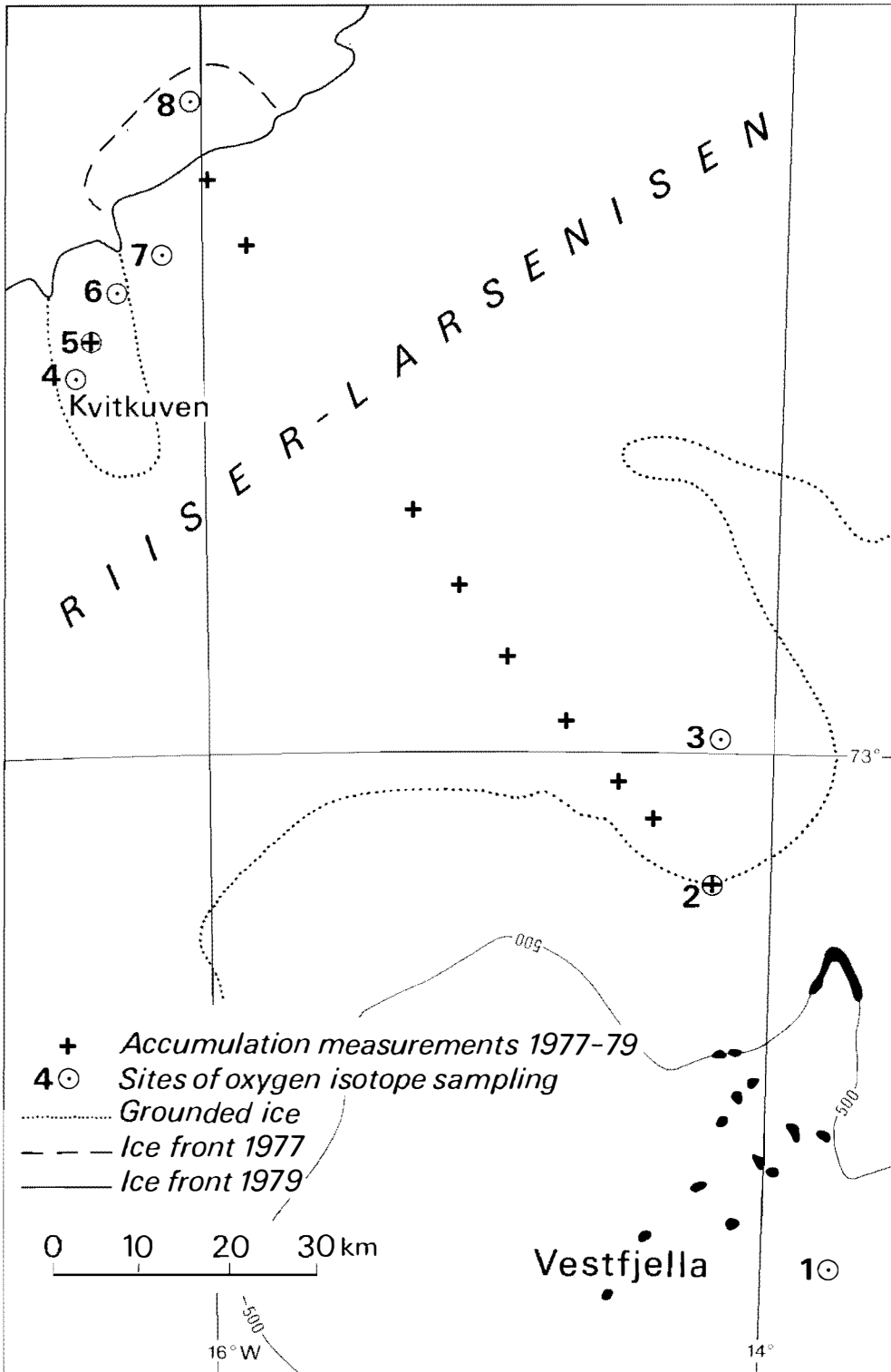
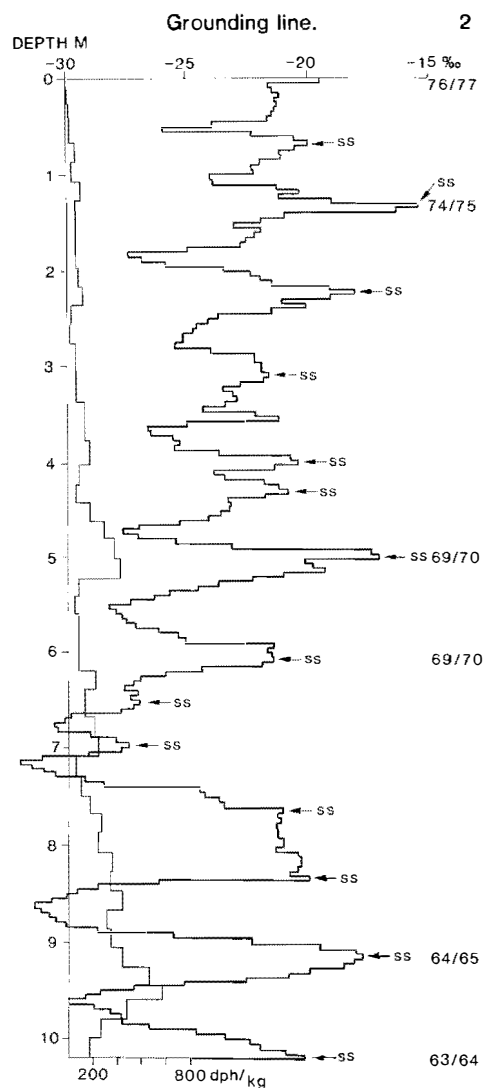
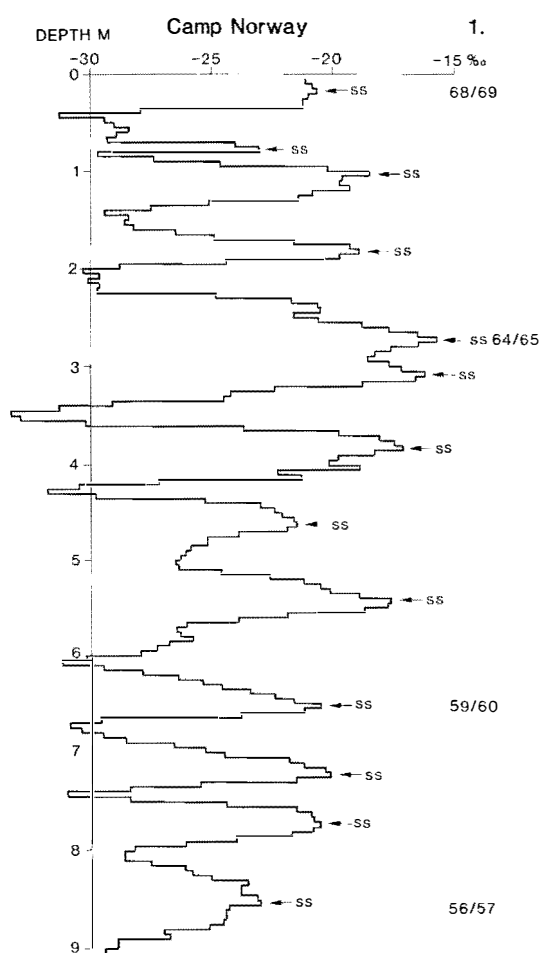


Fig. 2. Location of sampling sites 1-8, and of stakes for accumulation measurements (Gjessing & Wold 1986).

Table 1.  $\delta^{18}\text{O}$  samples from Riiser-Larsenisen.

No	Season	Locality	Total depth of core/samples (m)	Years	Total depth of stratigraphy (m)	Sites of strat. studies
1	1968/69	Camp Norway 1	9.1	12	8.5	
2	76/77	Grounding line	10.2	13	2.1	x
3	68/69	On shelf, 10 km from gr.line	4.4	5	5.5	
4	76/77	SW on Kvitkuven	10.95	20	1.5	x
5	76/77	Top of Kvitkuven	11.3	20	1.6	(x)
6	76/77	NE on Kvitkuven	13.35	20	1.2	x
7	78/79	3 km from Kvitkuven/shelf edge	13.0	17	2.1	
8	76/77	Camp Norway 3	4.0	5	3.5	x

Fig. 3.  $\delta^{18}\text{O}$  variations at site 1. 'SS' = summer surface on this and following Figs.Fig. 4.  $\delta^{18}\text{O}$  and total  $\beta$ -activity at site 2.

Specific total  $\beta$ -activity was not measured on the two sections collected in 1968/69. Thus, there are more uncertainties in the interpretation of these profiles. Nor are the  $\beta$ -activity variations adequate to give a dateable horizon for the short section, No. 8. For the others, the main uncertainties are concerned with the interpretation for the pre-1964 period. However, alternative identifications of annual layers are possible for sections dated by  $\beta$ -activity, at locations 5 and 7.

The alternative interpretation at location 5 (Fig. 7) would probably only change the balances for two years in the core and not affect the average values after 1964.

The core from location 7 (Fig. 9) presents a greater problem. Here the high  $\beta$ -activity at 5 m depth corresponds to the 1964/65-level in other cores, but this is not possible from the  $\delta$ -variations. One alternative interpretation to the one presented is that the core section from 4.2 m to 13 m was reversed in the field, i.e. that the 4.2 m level represents the base of the core and dates back to 1964. This interpretation would make the isotopic records more reasonable and would give a mean annual accumulation of 0.45 m w.eq., which is practically equal to the given interpretation. We think this explanation is the most likely one, but unfortunately we have no way of ascer-

taining whether such a reversal occurred. If the shown interpretation is correct, then the  $\beta$ -activity at 5 m is a local effect in the 1971 precipitation, and we note that the *mean*  $\beta$ -activity for that year is not unreasonably high.

The well-developed seasonal variations in this area with a mean annual accumulation  $>0.3$  m water equivalent (see below) imply that seasonal variations can be expected to survive metamor-

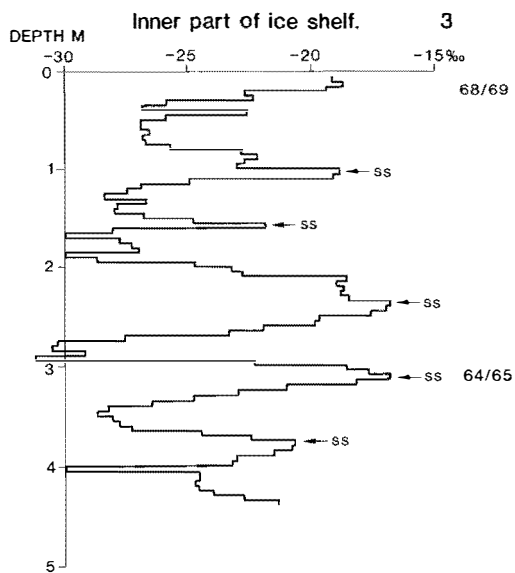


Fig. 5.  $\delta^{18}\text{O}$  variations at site 3.

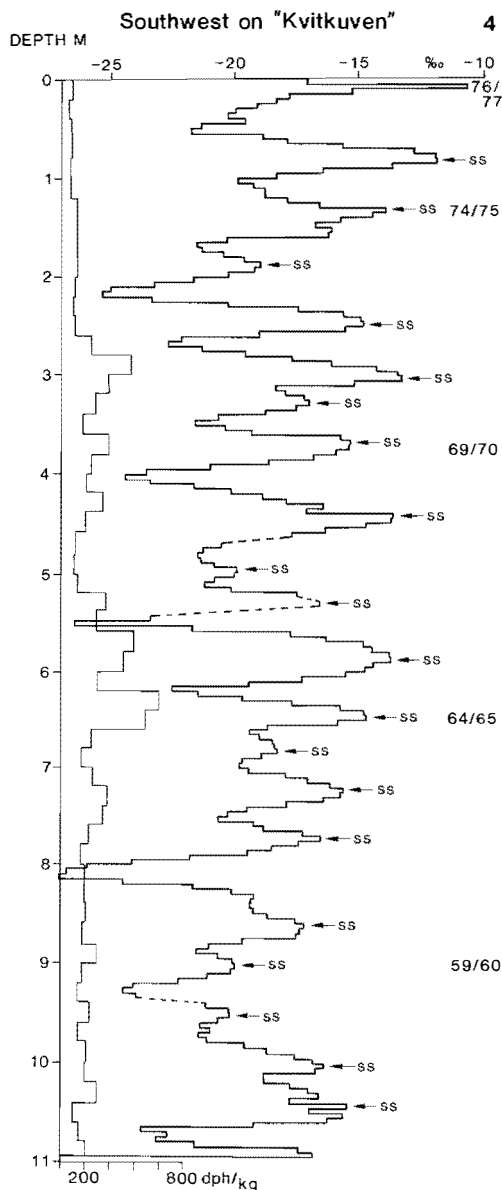


Fig. 6.  $\delta^{18}\text{O}$  and total  $\beta$ -activity at site 4.

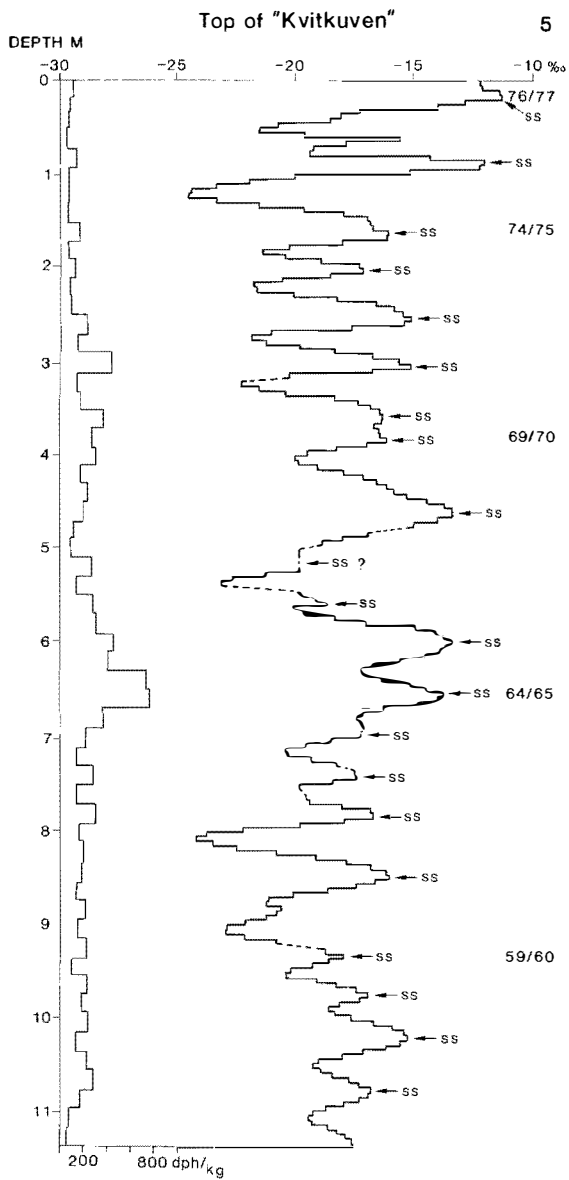


Fig. 7.  $\delta^{18}\text{O}$  and total  $\beta$ -activity at site 5.

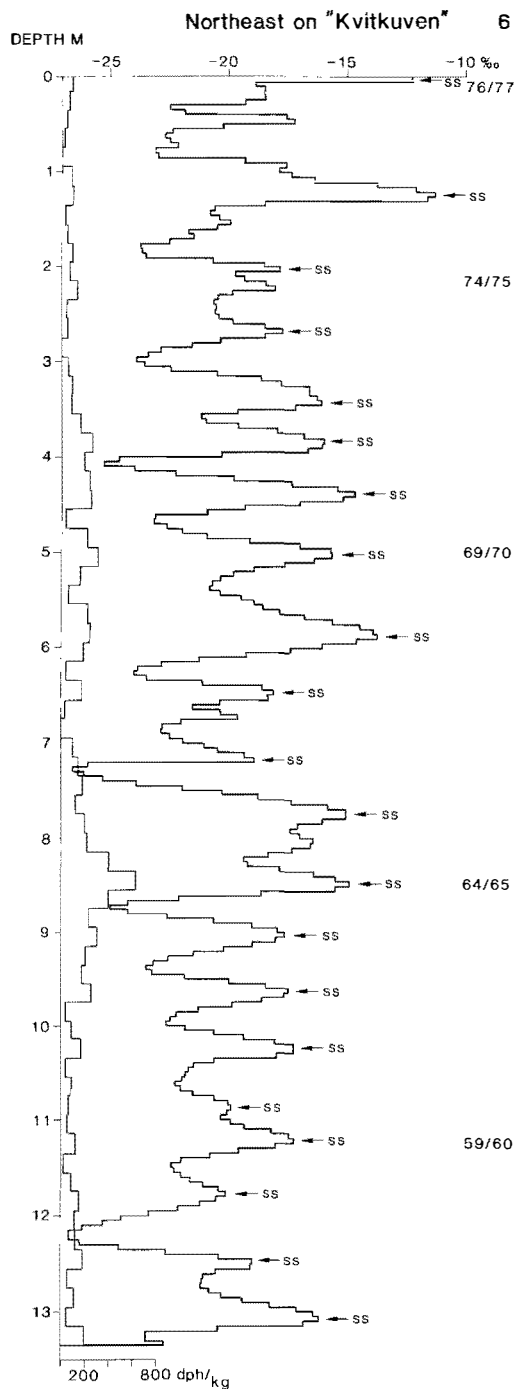


Fig. 8.  $\delta^{18}\text{O}$  and total  $\beta$ -activity at site 6.

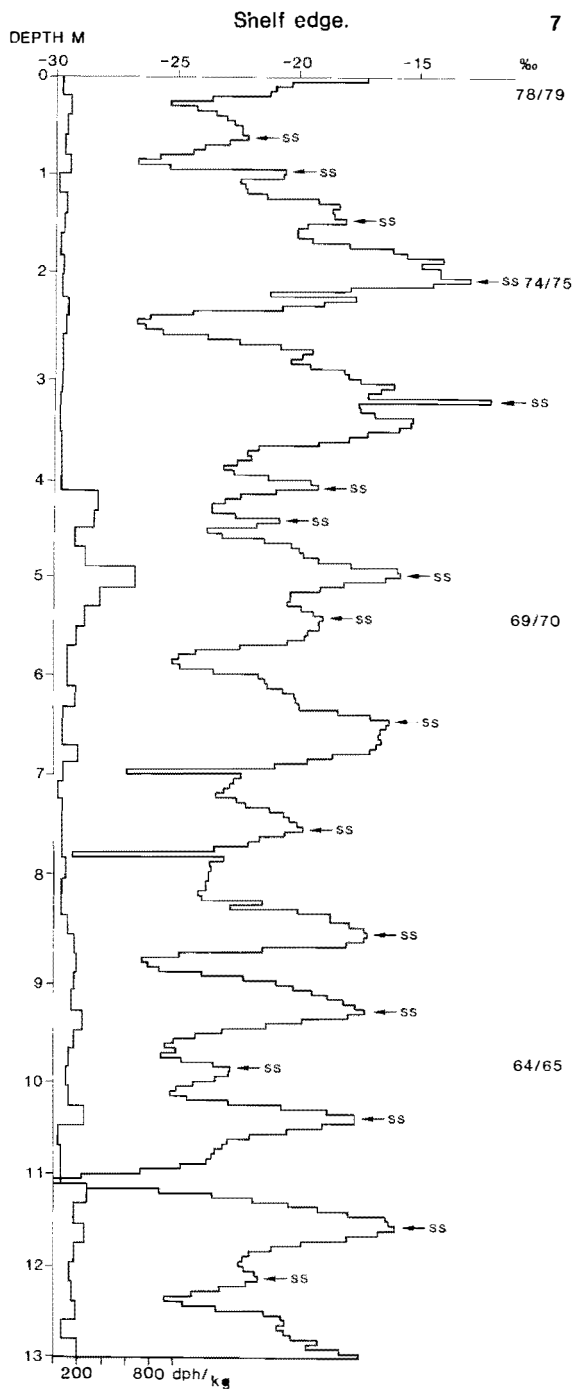


Fig. 9.  $\delta^{18}\text{O}$  and total  $\beta$ -activity at site 7.

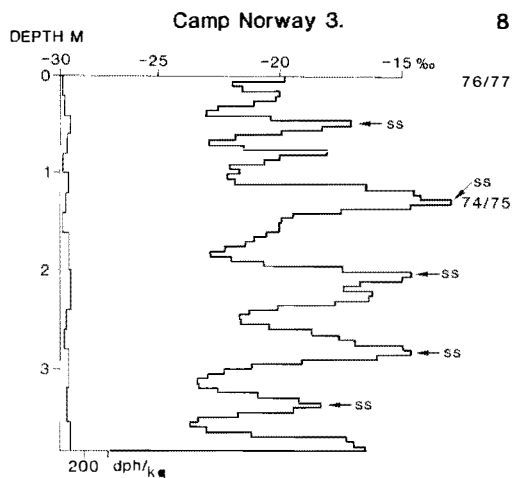


Fig. 10.  $\delta^{18}\text{O}$  and total  $\beta$ -activity at site 8.

phism, and be better preserved at depth than at most of the other locations in Antarctica where  $\delta^{18}\text{O}$  measurements have been made (e.g. Dansgaard et al. 1973; Johnsen 1977). This would therefore be a suitable area for deeper drillings with respect to potential dating of the ice core by  $\delta$ -variations and thus for studies of past climatic variations. The ice shelf varies in thickness from 200 m to 600 m (Orheim 1986), and a section from the thicker areas can be expected to extend to  $\approx 2000$  B.P. The detailed stratigraphic studies done by Repp (1978) at some of the localities (Table 1) show that the snow is wetted in the summer, refreezing to form ice layers, but that the annual layer is not soaked. Thus, most of the stratigraphy is not affected by melting and refreezing processes.

*Mean net balance*

The variations in annual accumulation at each site are presented in Fig. 11 and Table 2. The values are based on the identification of depths of summer surfaces presented in Figs. 3–10. The main errors, in addition to possible misidentification of annual layers, are related to 1) the depth resolution and 2) uncertainties in density.

The sampling interval of 0.05 m for the oxygen isotopes results in a possible error of 0.1 m in the thickness of an annual layer, or about 0.05 m water equivalent.

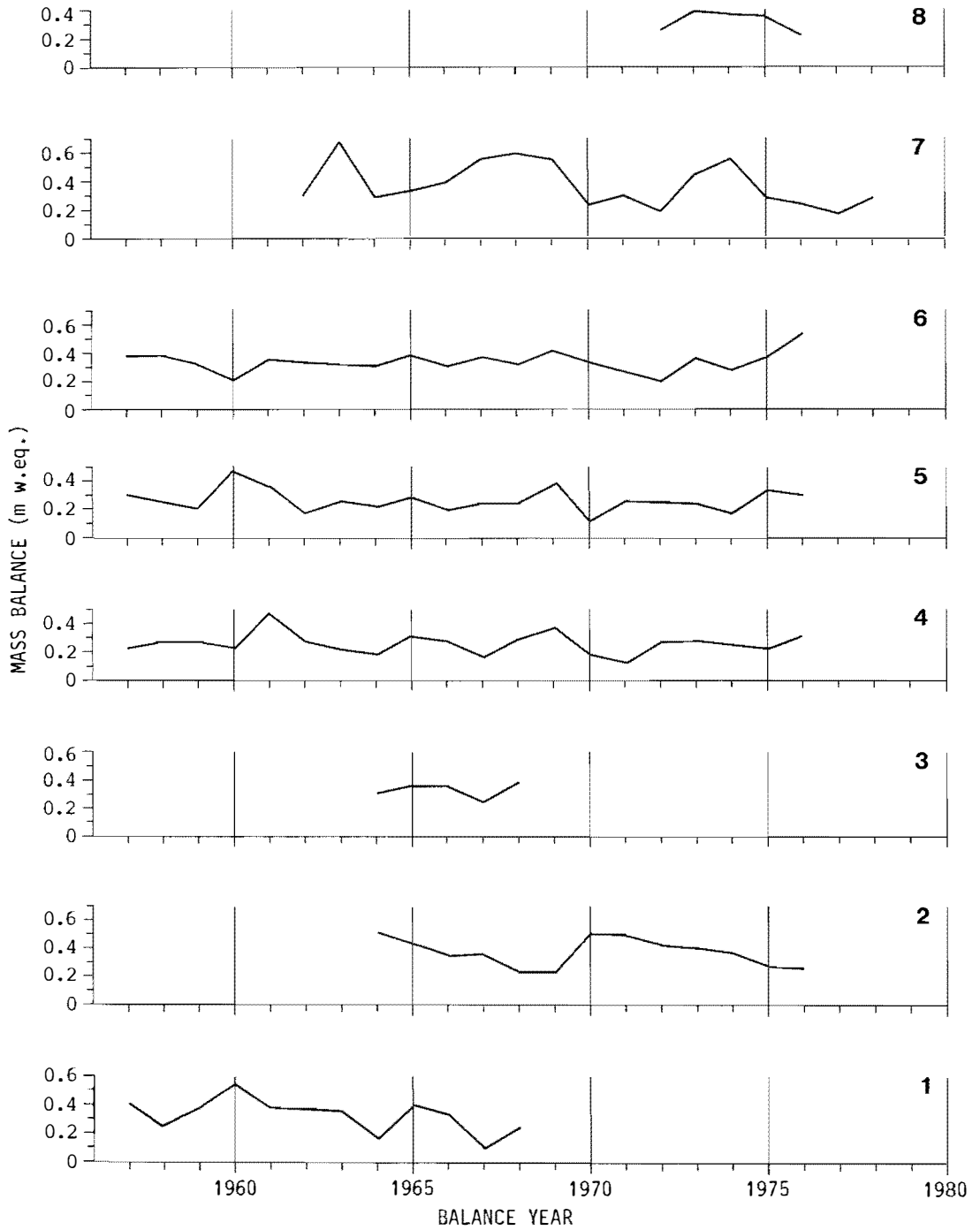


Fig. 11. Mean annual balance variations at sites 1-8.

Table 2. Mass balance in m water equivalents.

Year	1	2	3	4	5	6	7	8	Average
1978							0.28		
77							0.16		
76		0.28		0.32	0.30	0.55	0.23	0.22	0.32
75		0.29		0.23	0.34	0.37	0.27	0.35	0.31
74		0.39		0.25	0.18	0.29	0.54	0.37	0.34
73		0.42		0.28	0.24	0.37	0.44	0.39	0.36
72		0.44		0.27	0.25	0.20	0.18	0.30	0.27
71		0.52		0.13	0.27	0.27	0.29		0.30
70		0.54		0.19	0.12	0.34	0.22		0.28
69		0.24		0.38	0.39	0.41	0.54		0.39
68	0.26	0.24	0.39	0.29	0.25	0.32	0.58		0.33
67	0.11	0.37	0.25	0.16	0.25	0.37	0.54		0.29
66	0.36	0.35	0.37	0.27	0.19	0.30	0.38		0.32
65	0.43	0.45	0.37	0.32	0.29	0.39	0.32		0.37
64	0.17	0.53	0.32	0.19	0.22	0.31	0.28		0.29
63	0.37			0.21	0.27	0.32	0.67		0.37
62	0.40			0.27	0.18	0.34	0.29		0.30
61	0.40			0.48	0.36	0.36			0.40
60	0.56			0.22	0.47	0.20			0.36
59	0.38			0.27	0.20	0.32			0.29
58	0.26			0.27	0.25	0.38			0.29
57	0.43			0.23	0.31	0.37			0.34
Standard deviation	0.124	0.106	0.057	0.078	0.081	0.075	0.156	0.068	0.052
Mean 1965-76		0.378		0.258	0.256	0.348	0.378		0.323
Mean 1971-76		0.390		0.247	0.263	0.342	0.325		0.313
Mean 1965-70		0.365		0.268	0.248	0.355	0.430		0.333
Mean all years	0.344	0.389	0.340	0.262	0.267	0.339	0.365	0.326	0.322

The density values used are shown in Fig. 12. Density measurements were only collected to 4.0 m depth at Riiser-Larsenisen (Repp 1978). Here we have used his data for the first 3 m, and below that the average densities measured by Lunde (1961) at Norway Station. This gives a smooth curve which is intermediate among the various density-depth data collected from this region. They are all given in Fig. 12. Replacing the density values with those from either Halley or Maudheim, would change the total mass for the longest sections by about 0.2 m water equivalent, and for individual years by maximum 0.03 m. The errors resulting from the assumed density

curve are therefore not likely to be large. There are, of course, in reality large deviations from the smooth density/depth curve, especially for the near-surface layers (e.g. Schytt 1958). Thus, application of the above mentioned density curve probably reduces some of the real variability in annual accumulation, but without significantly affecting the multi-year means.

Although similar year-to-year variations can be recognized in several of the curves (Fig. 11), it is unlikely that the curves should parallel each other over longer periods. Considerable natural variation in accumulation can be expected, due to various effects including small scale surface

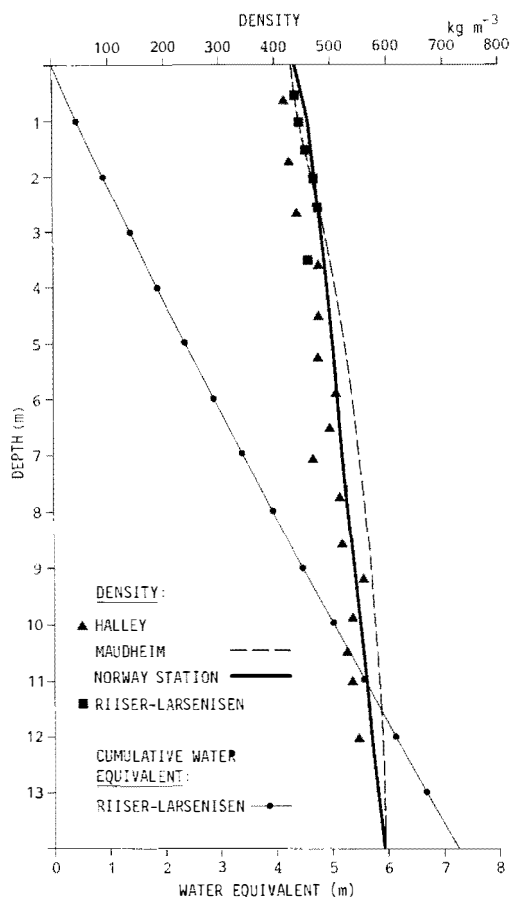


Fig. 12. Cumulative water equivalents at Riiser-Larsenisen, based on Repp's (1978) density measurements to 3 m depth and below that on smooth density curve from Norway Station (Lunde 1961). Also shown are the density variations with depth at Maudheim (Schytt 1958) and Halley (MacDowall 1964).

roughness, although such variations are comparatively greater in areas of low accumulation (e.g. Palais et al. 1982). The standard deviations presented in Table 2 show that the greatest variability in accumulation is shown at the long section from the coast (7). Comparatively great variability is also shown at the inland site (1) and at the grounding line (2). The Kvitkuven sites (4-6) show much smaller year-to-year variations, and the data also indicate lower mean accumulation on Kvitkuven, which is what would be expected from the topography.

Table 2 also shows the mean annual accumulation for individual locations and periods. The mean annual accumulation for all locations for the 22 accumulation years from 1957 to 1978 is 0.322 m of water equivalent. Excluding sample 1 located upstream from Riiser-Larsenisen, this gives a mean balance for the seven locations on the ice shelf of 0.319 m. There is no evidence of trends in mean balance for the time periods dated by total  $\beta$ -activity.

Table 3 compares the mean net balance as calculated from the isotope results with the balances determined by stratigraphic methods and from two years of stake measurements (Lunde, pers. comm.; Repp 1978; Gjessing & Wold 1986). It appears that the stratigraphic interpretation in 1976/77 overestimated the accumulation rate, whereas the 1968/69 work possibly underestimated the accumulation. The stake measurements for 1977/79 show considerably larger values than the multi-year mean accumulation determined from the studies at the same sites.

Table 3. Comparison mean net balances in m water equivalents.

Locality No	$b_n$	$\delta^{18}O$ Period	(years)	$b_n$	Stratigraphy Period	(years)	Stakes 1978-79
1	0.345	1957-68	(12)	0.215	1950-68	(19)	
2	0.389	1964-76	(13)	0.491	1975-76	(2)	0.583
3	0.340	1964-68	(5)	0.226	1958-68	(11)	0.584
4	0.262	1957-76	(20)	0.655	1976	(1)	
5	0.267	1957-76	(20)	0.665	1976	(1)	0.416
6	0.339	1957-76	(20)	0.515	1976	(1)	
7	0.365	1962-78	(17)	0.508	1977-78	(2)	
8	0.326	1972-76	(5)	0.539	1974-76	(3)	

The period shows the balance years determined, i.e. '1976' corresponds to the period between the 1975/76 and 1976/77 summer surfaces. The stratigraphic interpretations are from Lunde (locality 1, 3), Repp (2, 4, 5, 6, 8), and Wold (7); the last is more tentative.

Such differences between short and long-term measurements are not unusual, and the data probably reflect real differences for the different periods. It is noteworthy that the Halley data (Fig. 13) also show above-average accumulations for these two years.

Fig. 13 shows the mean annual accumulation at Riiser-Larsenisen together with records from Halley and SANAE/Norway Station. There is no statistically significant year-to-year correlation between the curves. Comparison of the results from near the ice front (7) with the long records from the nearby stations (also all located near the ice front) indicates that the mean accumulation does not vary significantly with latitude along the coast: 0.495 m and 0.374 m at Norway Station and SANAE (Lunde 1961; Neethling 1970), 0.365 m at Maudheim (Schytt 1958), 0.365 m at Riiser-Larsenisen, and 0.382 m at Halley (compiled from data provided by Limbert, pers. comm.). This conclusion must be tempered by the fact that these records represent different periods and different techniques, but it agrees well with the balance map produced by Bull (1971).

#### $\delta$ -variations and temperatures

Table 4 shows the mean  $\delta$  for each site together with elevation and distance from the sea, and

mean annual temperatures based on snow temperatures at 10 m depth (Lunde, pers. comm.; Gjessing & Wold 1986). As expected, the mean annual temperature and  $\delta$  are correlated. Fig. 14 shows that the data fit well on the  $\delta$ /temperature curve from the Antarctic Peninsula discussed by Peel & Clausen (1982), with a steeper slope ( $1.3\text{‰}/^{\circ}\text{C}$ ) than in other parts of Antarctica.

Localities 4 and 5, on the ice rise Kvitkuven, are noticeable for having less negative  $\delta\text{O}^{18}$ . This suggests less winter accumulation, perhaps as a result of scouring (Fisher et. al. 1983). This is

Table 4. Mean  $\delta^{18}\text{O}$ , annual temperature, elevation, distance from sea,  $b_n$ .

No	Mean $\delta^{18}\text{O}$ ‰	Mean ann. temp. ° C	Elevation m	Dist. from sea km	Balance $b_n$ m
1	- 24.3	- 21.4	743	150	0.345
2	- 24.04	- 19.2	60	110	0.389
3	- 24.2	- 18.0	≈ 75	90	0.340
4	- 18.75		≈ 150	7	0.262
5	- 18.03	- 16.4	200	5	0.267
6	- 19.93	- 15.4	100	4	0.339
7	- 20.88	- 16.8	40	5	0.365
8	- 19.67		30	2	0.326

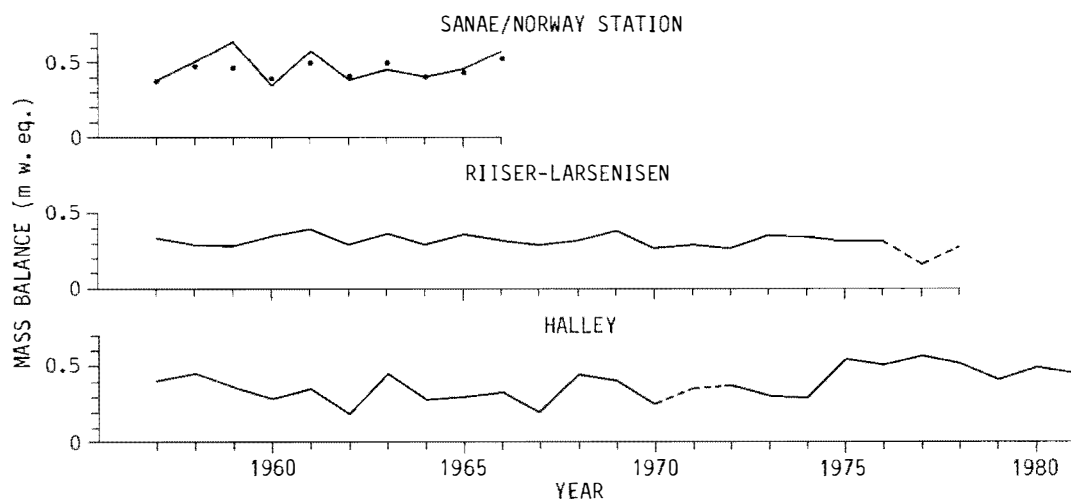


Fig. 13. Annual mass balance variations at Riiser-Larsenisen (Table 2) compared with Halley (Limbert, pers. comm.) and SANAE (Neethling 1970). The latter include results from both stratigraphy (dots) and stakes (solid line).

supported by the accumulation rates at these two localities, which are the lowest of the measured cores.

The  $\delta$ -concentration in precipitation has been measured at Halley since 1965. The 1965–75 monthly  $\delta$ -variations given by the International Atomic Energy Agency (1970, 1972, 1973, 1975, 1979) are shown in Fig. 15, and computations from the data in these publications give a mean  $\delta$  of  $-19.7\text{‰}$  and a mean air temperature of  $-18.3^\circ\text{C}$  for the nine complete years 1966, 1967

and 1969–75. The corresponding means for the five localities (2, 3, 5, 6, 7) on Riiser-Larsenisen for which both  $\delta$  and temperature data are available are  $-20.6\text{‰}$  and  $-17.2^\circ\text{C}$ . These series do not cover identical periods, but the data indicate that within the margins of uncertainty the mean conditions are very similar for these two areas. The mean temperature is probably lower than  $-18.3^\circ\text{C}$  at Halley. It was  $-19.3^\circ\text{C}$  for the years 1956–81 (computed from data provided by Limbert, pers. comm.).

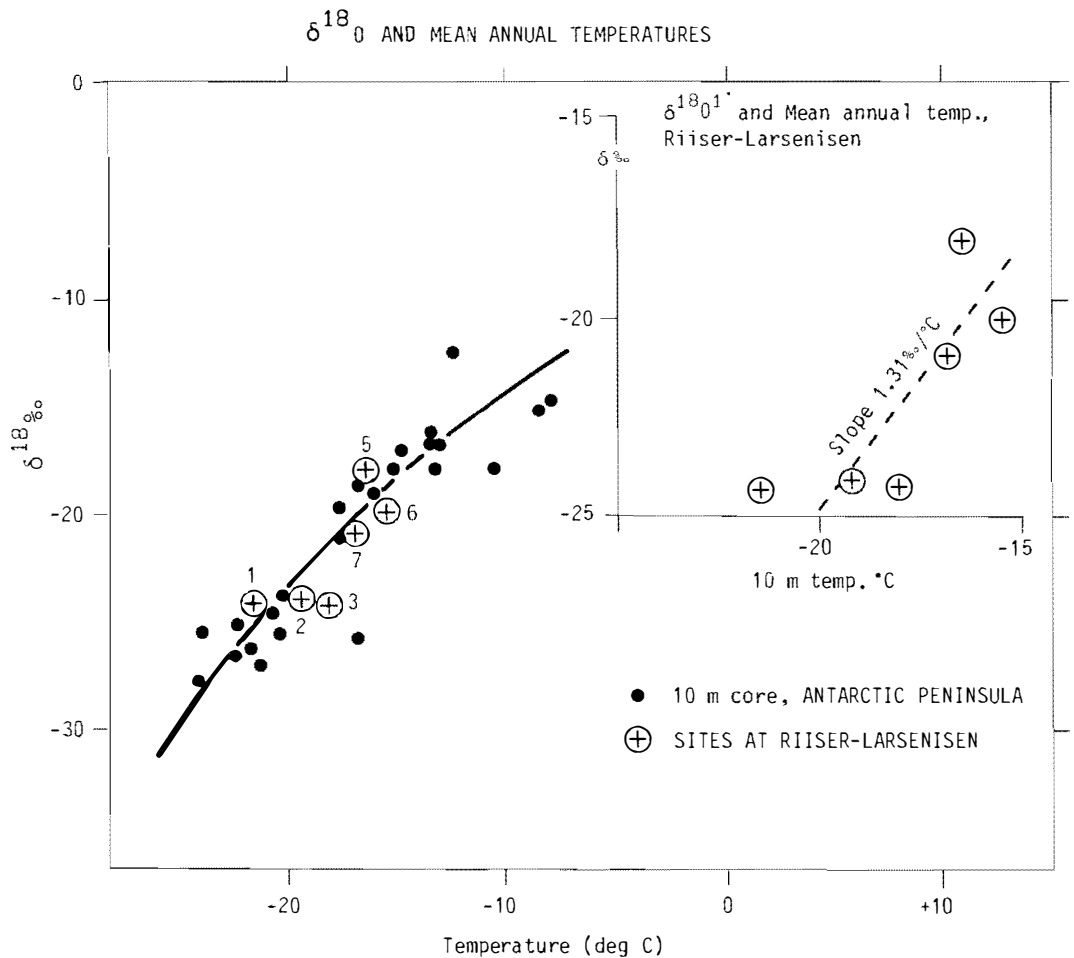


Fig. 14. Mean  $\delta$ -values plotted against mean annual temperatures (10 m) for the Riiser-Larsenisen sites and compared with data from the Antarctic Peninsula. (Peel & Clausen 1982).

The mean  $\delta$  for all sections on Riiser-Larsen is  $-20.2\text{‰}$ . Comparison between Fig. 15 and Figs. 3-10 shows larger monthly and seasonal variations at Halley. It is reasonable that the snow/firn sections should show lower variability than the precipitation data. There is considerable smoothing of the isotope profile through the vapour phase in the upper few metres. Furthermore, the snow samples may at times represent combinations of several precipitation events, including effects from post-depositional mixing,

and a 0.05 m sample may include precipitation from more than one month. In other cases adjoining samples may represent snow from the same precipitation event. These effects will cause smoothed profiles compared with the precipitation data.

*$\delta$ -variations at Fimbulisen*

Fig. 16 shows the variation in two cores collected at Fimbulisen in western Dronning Maud Land, at the coast not far from the present SANAE and

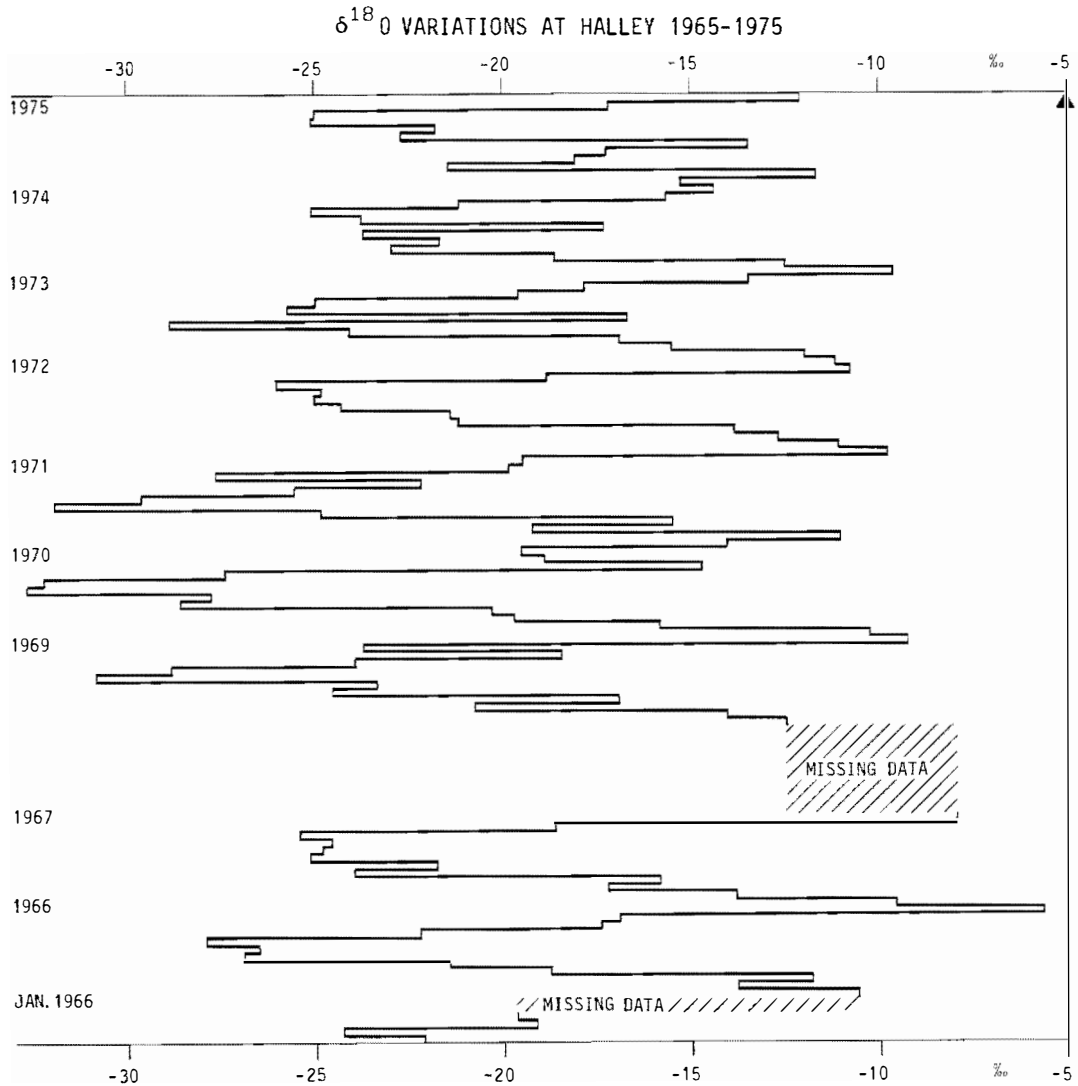


Fig. 15.  $\delta^{18}\text{O}$  concentration in precipitation measured at Halley from 1965 to 1975.

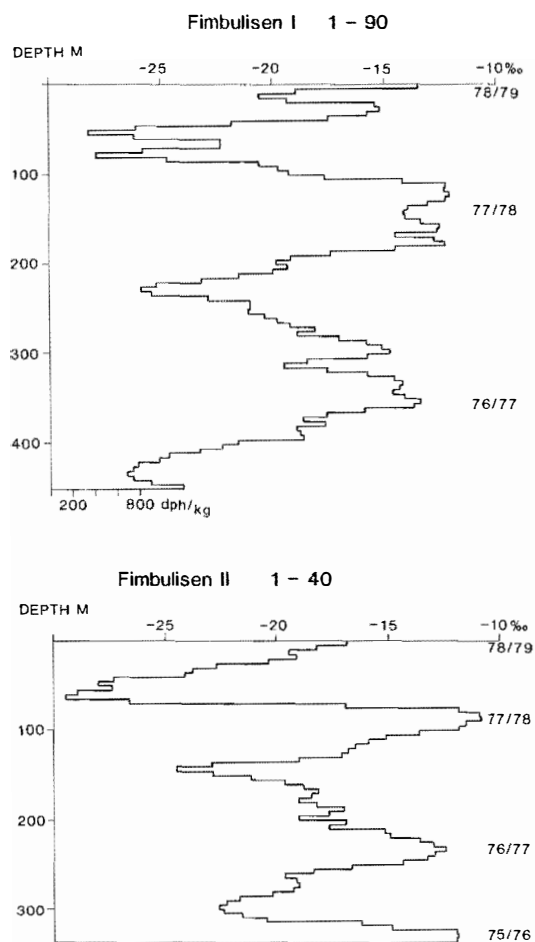


Fig. 16.  $\delta^{18}\text{O}$  variations at two locations at Fimbulisen, at approximately  $70^{\circ}00'\text{S}$ ,  $1^{\circ}25'\text{W}$  (Fig. 1).

former Norway Station (Fig. 1). The cores from Fimbulisen show larger  $\delta$ -variations than any of those at Riiser-Larsenisen, presumably because Fimbulisen experiences more variation in precipitating air masses. The mean  $\delta$  computed from the two complete balance years in each core is  $-18.1\text{‰}$  for Fimbulisen I and  $-17.3\text{‰}$  for Fimbulisen II. The  $\delta$ -variations indicate a mean balance for the two sites of 0.86 m and 0.55 m water equivalent, respectively.

## Conclusions

Oxygen isotope data of snow and firn samples from eight locations on and upstream of Riiser-Larsenisen show well-developed seasonal varia-

tions. These variations can be expected to be preserved with depth, making the area suitable for deeper drillings. The oldest sections extend back to 1957, and the 1964 and 1970 levels have been dated in five sections by total  $\beta$ -activity. The mean annual balance at Riiser-Larsenisen is 0.32 m water equivalent. It varies little across the ice shelf, apart from a somewhat lower accumulation on the ice rise Kvitkuven.

The mean annual mass balance at Riiser-Larsenisen is close to that recorded at the nearby Halley and Maudheim stations, indicating that the precipitation along the north-eastern coast of the Weddell Sea varies little with latitude.

The mean  $\delta^{18}\text{O}$  at Riiser-Larsenisen is  $-20.2\text{‰}$ , compared with  $-19.7\text{‰}$  for precipitation measured at Halley. Comparisons of  $\delta$ -variations and mean annual temperatures indicate a relationship close to that found for the Antarctic Peninsula, and a somewhat greater change with temperature than described elsewhere in Antarctica.

There is no statistically significant correlation between the annual mass balance variations at the different sampling sites, or between the mean annual balances from Riiser-Larsenisen and the annual balances at Halley and SANAE.

## Acknowledgements

We would like to thank various expedition members of NARE 1976/77 and 1978/79 for helpful assistance in the field.

## References

- Bull, C. 1971: Snow accumulation in Antarctica. Pp. 367-421 in Quam, Q.L. (ed.): Research in the Antarctic. *American Ass. for Advancement of Science* 93.
- Clausen, H.B. & Dansgaard, W. 1977: Less surface accumulation on the Ross Ice Shelf than hitherto assumed. IUGG/IASH Symposium on isotopes and impurities in snow and ice, Grenoble, 28-30 August 1975. *IASH* 118, 172-176.
- Craig, H. 1961: Standard for reporting concentrations of deuterium and oxygen-18 in natural waters. *Science* 133, 1833-1834.
- Dansgaard, W., Johnsen, S.J., Clausen, H.B. & Gundestrup, N. 1973: Stable isotope glaciology. *Meddelelser om Grønland* 197(2), 53 pp.
- Fisher, D.A., Koerner, R.M., Paterson, W.S.B., Dansgaard, W., Gundestrup, N. & Reeh, N. 1983: Effect of wind scouring on climatic records from ice-core oxygen-isotope profiles. *Nature* 301, 205-209.

- Gjessing, Y. 1984: Antropogenic and marine contributions to the chemical composition of snow at Riiser-Larsenisen in Antarctica. *Atmospheric Environment* 18(4), 825–830.
- Gjessing, Y. & Wold, B. 1986: Absolute movements, mass balance and snow temperatures of Riiser-Larsenisen, Antarctica. *Norsk Polarinstitutt Skrifter*, 187, 23–31 (this volume).
- International Atomic Energy Agency 1970: Environmental isotope data No. 2. World survey of isotope concentration in precipitation (1964–65). *Technical report series 117*. IAEA, Vienna.
- International Atomic Energy Agency 1972: Environmental isotope data No. 3. World survey of isotope concentration in precipitation (1966–67). *Technical report series 129*. IAEA, Vienna.
- International Atomic Energy Agency 1973: Environmental isotope data No. 4. World survey of isotope concentration in precipitation (1968–69). *Technical report series 147*. IAEA, Vienna.
- International Atomic Energy Agency 1975: Environmental isotope data No. 5. World survey of isotope concentration in precipitation (1970–71). *Technical report series 165*. IAEA, Vienna.
- International Atomic Energy Agency 1979: Environmental isotope data No. 5. World survey of isotope concentration in precipitation (1972–75). *Technical report series 192*. IAEA, Vienna.
- Johnsen, S.J. 1977: Stable isotope homogenization in polar firn and ice. IUGG/IASH Symposium on isotopes and impurities in snow and ice, Grenoble, 28–30 August 1975. *IASH 118*, 210–219.
- Lunde, T. 1961: On the snow accumulation in Dronning Maud Land. *Norsk Polarinstitutt Skrifter* 123, 48 pp.
- MacDowall, J. 1964: Glaciological observations. Part I. Glaciological observations at the base. Pp. 269–313 in Brunt, D. (ed.): *The Royal Society International Geophysical Year Antarctic Expedition, Halley Bay, Coats Land, Falkland Islands Dependencies, 1955–59. IV*. Royal Society, London.
- Neethling, D.C. 1970: Snow accumulation on the Fimbul Ice Shelf, western Dronning Maud Land, Antarctica. Pp. 390–404 in Gow, A.J., Keeler, C., Langway, C.C. & Weeks, W.F. (eds.): International Symposium on Antarctic Glaciological Exploration (ISAGE). *IASH 86*, and *SCAR*. Cambridge.
- Orheim, O. 1986: Flow and thickness of Riiser-Larsenisen. *Norsk Polarinstitutt Skrifter* 187, 5–22 (this volume).
- Palais, J.M., Whillans, I.M. & Bull, C. 1982: Snow stratigraphic studies at Dome C, East Antarctica: An investigation of depositional and diagenetic processes. *Annals of Glaciology* 3, 239–242.
- Peel, D.A. & Clausen, H.B. 1982: Oxygen-isotope and total beta-radioactivity measurements on 10 m ice cores from the Antarctic Peninsula. *Journal of Glaciology* 28, 43–55.
- Picciotto, E., Crozaz, G. & DeBreuck, W. 1971: Accumulation on the South Pole – Queen Maud Land Traverse, 1964–1968. Pp. 257–315 in Crary, A.P. (ed.): *Antarctic Research Series 16, Antarctic Snow and Ice Studies II*. American Geophysical Union, Washington.
- Picciotto, E. & Wilgain, S.E. 1963: Fission products in Antarctic snow, a reference level for measuring accumulation. *Journal of Geophysical Research* 68, 5965–5972.
- Repp, K. 1978: Snow accumulation and snow stratigraphy on Riiser-Larsenisen, Dronning Maud Land, Antarctica. *Norsk Polarinstitutt Skrifter* 169, 81–92.
- Schytt, V. 1958: Glaciology. A. Snow Studies at Maudheim. *Norwegian-British-Swedish Antarctic Expedition, 1949–52. Scientific Results IV (II)*, 1–63.

